AD

USAAVLABS TECHNICAL REPORT 69-3

MAXIMUM LOAD PREDICTION FOR SANDWICH PLATES

By

J. Mayers

Yuan-shan Chu

April 1969

U. S. ARMY AVIATION MATERIEL LABORATORIES
FORT EUSTIS, VIRGINIA

CONTRACT DAAJ02-68-C-0035
STANFORD UNIVERSITY
STANFORD, CALIFORNIA

DISCLAIMERS

The findings in this report are not to be construed as an official Department of the Army position unless so designated by other authorized documents.

When Government drawings, specifications, or other data are used for any purpose other than in connection with a definitely related Government procurement operation, the United States Government thereby incurs no responsibility nor any obligation whatsoever; and the fact that the Government may have formulated, furnished, or in any way supplied the said drawings, specifications, or other data is not to be regarded by implication or otherwise as in any manner licensing the holder or any other person or corporation, or conveying any rights or permission, to manufacture, use, or sell any patented invention that may in any way be related thereto.

DISPOSITION INSTRUCTIONS

Destroy this report when no longer needed. Do not return it to the originator.

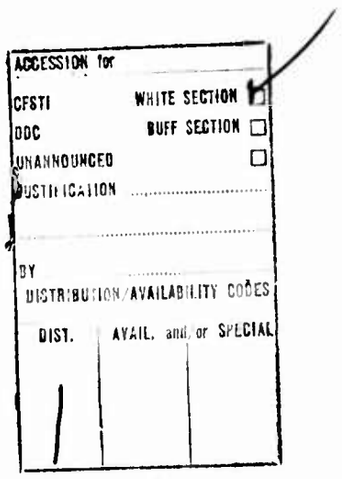

DEPARTMENT OF THE ARMY
U. S. ARMY AVIATION MATERIEL LABORATORIES
FORT EUSTIS, VIRGINIA 23604

This program was carried out under Contract DAAJ02-68-C-0035 with Stanford University.

The data contained in this report are the result of research conducted to assess the effects of transverse shear deformation on the maximum strength of sandwich plates when the primary mode of initial buckling is that of general instability.

The report has been reviewed by the U. S. Army Aviation Materiel Laboratories and is considered to be technically sound. It is published for the exchange of information and the stimulation of future research.

Task 1F162204A17002
Contract DAAJ02-68-C-0035
USAAVLABS Technical Report 69-3
April 1969

MAXIMUM LOAD PREDICTION FOR SANDWICH PLATES

By

J. Mayers and Yuan-shan Chu

Prepared by
Stanford University
Stanford, California

For
U.S. ARMY AVIATION MATERIEL LABORATORIES
FORT EUSTIS, VIRGINIA

SUMMARY

An investigation of the postbuckling behavior of sandwich plates compressed beyond the general instability load into the plastic range has been undertaken. The study is a natural extension of previous work which led to the establishment of maximum load-prediction capability relative to conventional plates. The purpose of the present investigation is to assess the effects of transverse shear deformations on the maximum strength of sandwich plates when the primary mode of initial buckling is that of general instability. The analysis utilizes a modified version of Reissner's variational principle and a deformation theory of plasticity in conjunction with computations carried out on high-speed computing equipment. The results indicate that for the particular plate problem investigated (for example, aircraft wing or stabilizer plate element), the postbuckling load-carrying capability is essentially independent of transverse shear effects in the presence of inelastic behavior of the sandwich faces. The implication is that perhaps designers will not have to be as conservative in sizing sandwich plate sections for maximum load-carrying capability as purely elastic theory results would indicate.

FOREWORD

The work reported herein constitutes a portion of a continuing effort being undertaken at Stanford University for the U.S. Army Aviation Materiel Laboratories under Contract DAAJ02-68-C-0035 (Task 1F162204A17002) to establish accurate theoretical prediction capability for the static and dynamic behavior of aircraft structural components utilizing both conventional and unconventional materials. Predecessor contracts supported investigations which led, in part, to the results presented in References 2,3,5,6, and 8.

TABLE OF CONTENTS

	Page
SUMMARY	iii
FOREWORD	v
LIST OF ILLUSTRATIONS	viii
LIST OF SYMBOLS	ix
INTRODUCTION	1
PROBLEM DESCRIPTION AND GENERAL THEORY	2
Statement of the Problem	2
General Theory	3
METHOD OF SOLUTION	5
Elastic Solution	5
Plastic Solution	6
RESULTS AND DISCUSSION	8
CONCLUDING REMARKS	9
LITERATURE CITED	17
APPENDIXES	
I. Euler Equations and Boundary Conditions Derived from Variational Principle	18
II. Elastic Analysis	25
III. Plastic Analysis and Newton-Raphson Iterative Technique	33
IV. Effective Stress and Strain	38
DISTRIBUTION	40

LIST OF ILLUSTRATIONS

Figure		Page
1	Plate Geometry and Coordinate System	10
2	Compressive Stress-Strain Curve and Initial Buckling Stresses for 2024-T3 Aluminum-Alloy Plates Analyzed. (From Reference 1, Figure 2.)	11
3	Variation of $N_x/(N_{xo})_{cr}$ Across Plate at Any Cross Section .	12
4	Variation of $(N_x)_{av}/(N_{xo})_{cr}$ with $\bar{u}/\bar{u}_{cr}$ for Several Values of the Transverse Shear Stiffness Parameter γ	13
5	Variation of w_{max}/h with $\bar{u}/\bar{u}_{cr}$ for Several Values of the Transverse Shear Stiffness Parameter γ	14
6	Variation of $(N_x)_{av}/(N_{xo})_{cr}$ with $\bar{u}/\bar{u}_{cr}$, Plate 1, σ_{cr}/σ_{cy} = 0.6.	15
7	Variation of $(N_x)_{av}/(N_{xo})_{cr}$ with u/u_{cr}, Plate 4, σ_{cr}/σ_{cy} = 0.3.	16

LIST OF SYMBOLS

b	plate dimension in y-direction, in.
$\overline{C}$	arbitrary displacement coefficient, in.
$\widetilde{C}$	arbitrary nondimensional displacement coefficient
$\overline{D},\overline{E}$	arbitrary shear strain coefficients, in./in.
$\widetilde{D},\widetilde{E}$	arbitrary nondimensional shear strain coefficients
D_Q	transverse shear stiffness, $D_Q = G_c t_c$, lb/in.
D_s	flexural rigidity of two-element plate, $D_s = 2Et_f \cdot h^2/3$, $(\mu = \frac{1}{2})$, lb/in.
E	Young's modulus for facing material, $lb/in.^2$
F'	complementary energy density, $lb/in.^2$
$\overline{F},\overline{G}$	arbitrary load coefficients, lb/in.
$\widetilde{F},\widetilde{G}$	arbitrary nondimensional load coefficients
G_c	shear modulus of the core material, $lb/in.^2$
h	distance between middle surfaces of facings, in.
$\overline{I},\overline{J}$	arbitrary bending moment coefficients, lb-in./in.
$\widetilde{I},\widetilde{J}$	arbitrary nondimensional bending moment coefficients
K	material constant
$\overline{K}$	arbitrary twisting moment coefficient, lb-in./in.
$\widetilde{K}$	arbitrary nondimensional twisting moment coefficient
k_x	nondimensional load parameter, $k_x = N_{xo}b^2/D_s\pi^2$
L	plate dimension in x-direction, in.
M_x,M_y	bending moments per unit length, lb-in./in.
M_{xy}	twisting moment per unit length, lb-in./in.
m,n	integers

N_x, N_y inplane compressive forces per unit length in x- and y-directions, respectively, lb/in.

N_{xy} inplane shear force per unit length, lb/in.

N_{xo} arbitrary force coefficient, lb/in.

$\tilde{N}_{xo}$ arbitrary nondimensional force coefficient

n material constant

t_c thickness of core, in.

t_f thickness of one facing, in.

U'' Reissner functional, lb-in.

$\bar{U}''$ nondimensional Reissner functional

$\bar{u}$ unit end shortening applied to plate, in./in.

u,v,w displacement of point in middle surface in x-, y- and z-directions, respectively, in.

V total volume of plate, $V = 2t_f Lb$, $in.^3$

β buckle aspect ratio, $\beta = mb/nL$

γ nondimensional shear stiffness parameter, $\gamma = D_s\pi^2/D_Q b^2$

γ'_{xy} shearing strain at middle surface, in./in.

γ''_{xy} shearing strain due to twisting, in./in.

γ_{xy}, γ_{yz} shearing strain in xz- and yz-planes, respectively, in./in.

ϵ_{eff} effective strain, $\epsilon_{eff} = \frac{2}{\sqrt{3}} \sqrt{\epsilon_x^2 + \epsilon_y^2 + \epsilon_x\epsilon_y + (\gamma_{xy}^2/4)}$, in./in.

ϵ_x, ϵ_y components of strain in x- and y-directions, respectively, in./in.

ϵ'_x, ϵ'_y inplane strain at middle surface, in./in.

$\epsilon''_x, \epsilon''_y$ bending strain, in./in.

η nondimensional lateral coordinate, $\eta = 2ny/b$

μ	Poisson's ratio
ξ	nondimensional axial coordinate, $\xi = 2mx/L$
σ_{eff}	effective stress, $\sigma_{eff} = \sqrt{\sigma_x^2 + \sigma_y^2 - \sigma_x\sigma_y + 3\tau_{xy}^2}$, lb/in.^{2}
σ_x, σ_y	components of stress in x- and y-directions, respectively, lb/in.^{2}
σ'_x, σ'_y	local average stress, lb/in.^{2}
σ''_x, σ''_y	bending stress, lb/in.^{2}
τ_{xy}	total shear stress in xy-plane, lb/in.^{2}
τ'_{xy}	local average shear stress, lb/in.^{2}
τ''_{xy}	shear stress due to twisting, lb/in.^{2}
τ_{xy}, τ_{yz}	transverse shear stress in xy- and yz-planes, respectively, lb/in.^{2}

Subscripts

av	average value
c	core
cr	critical value
cy	compressive yield
s	secant
t,b	top and bottom face, respectively

INTRODUCTION

The postbuckling and maximum strength analysis of square and rectangular plates has been carried out by Mayers et al.[1,2,3] with the use of a two-element model (see Figure 1). In Reference 3, Mayers and Nelson state: "The core separating the faces of the plate is considered rigid in shear in the present investigation, but provides a means to extend the current analysis to include transverse shear deformation when postbuckling behavior of sandwich plates is of interest." The objective and contributions of this report are to extend the earlier work and to establish the magnitude of the reduction in load-carrying ability of postbuckled sandwich plates due to transverse shear effects. The study of sandwich plate and shell behavior has been undertaken by Mayers et al. for over a period of almost twenty years (References 4,5, and 6). With ever-increasing interest being shown by designers in sandwich construction for primary structures in aerospace vehicles, a theoretical prediction capability is required. Although much progress has been made in stability analysis of sandwich structures, very little information is available for the prediction of maximum load-carrying capability. This report, then, may be considered as a small supplementary portion of a much greater research effort aimed at developing accurate prediction capability for the bending, buckling, post-buckling, and maximum strength of sandwich plates and shells. Most of the notations used here are the same as those in Reference 3. This makes it more convenient to compare the equations, expressions, and curves presented here with those appearing in References 1, 2, 3, and 7. These comparisons show the effects of transverse shear on the maximum load-carrying capability of infinitely long sandwich plates with a type of edge condition representative of aircraft wing panels. Although calculations have been carried out only for very long panels, the theoretical development presented herein is established for retangular plates in general. Thus, only the computational procedure must be applied to produce load-shortening curves for such plates. The results contained herein for long plates indicate that transverse shear effects reduce the postbuckling load-carrying capability to much the same degree of magnitude as does the phenomenon of buckle wavelength change in long conventional plates. The combination of postbuckling waveform modification, buckle wavelength change, and transverse shear flexibility leaves little postbuckling load-carrying capability in sandwich plates with relatively lightweight cores. For aircraft operating in the low and medium subsonic speed range, where some buckling of the wing surface is tolerable, only a more detailed comparison study can disclose which of the two types of plates (conventional or sandwich) is the more competitive on a maximum-strength-to-weight basis.

PROBLEM DESCRIPTION AND GENERAL THEORY

STATEMENT OF THE PROBLEM

The general problem considered here is the determination of the buckling and postbuckling behavior of the two-element rectangular sandwich plate shown in Figure 1. All of the four edges are simply supported, and both the loaded and unloaded edges are constrained to remain straight. A unit shortening is applied in the x-direction, which up to buckling corresponds to a uniform axial compression N_{xo}. For convenience and with justification obtained from the quantitative results of Reference 3, the translation of each point in the y-direction is assumed to be zero. The transverse shear flexibility of the core in the xz- and yz-planes is considered, thereby relaxing the rigid-core assumption inherent in References 1, 2, and 3. Material compressibility is neglected; thus, Poisson's ratio is taken as 0.5 throughout this development.

The material selected is 2024-T3 aluminum alloy (see Figure 2). For this aluminum alloy, the material constants in the Ramberg-Osgood uniaxial stress-strain curve representation

$$\epsilon = \frac{\sigma}{E} + K\left(\frac{\sigma}{E}\right)^n$$

are

$$K = 3.14 \times 10^{17}$$

$$n = 8.60$$

$$E = 10.7 \times 10^{6} \text{ psi}$$

with

$$\sigma_{cy} = 43.6 \text{ ksi.}$$

Two different plate cross-section geometries are studied. For the purpose of direct comparison with earlier work, the two-plate cross sections correspond to those of Reference 1, which are designated as

$$\text{plate 1:} \quad \sigma_{cr}/\sigma_{cy} = 0.6$$

and

$$\text{plate 4:} \quad \sigma_{cr}/\sigma_{cy} = 0.3.$$

The different plate critical stresses define different ratios of h/b. For each plate, the values of $\gamma = 0$, 0.25, and 0.5 are used to establish the required load-shortening curves. The curves for $\gamma = 0$ (equivalent to a core rigid in shear) are introduced so as to provide a check with the load-shortening curves for plates 1 and 4 (transverse shear effects neglected) in Reference 1. The main purpose of this research is to study the variation of $(N_x)_{av}/(N_{xo})_{cr}$ with u/u_{cr} in the postbuckling range to assess the magnitude of the reduction in postbuckling strength caused by finite shear flexibility of the core.

GENERAL THEORY

The basic problem is formulated in terms of a variational principle. As demonstrated in Reference 7, Reissner's variational principle is an alternative to the potential energy principle. In References 3 and 8, Reissner's principle is shown to be a better alternative than the potential energy principle for nonlinear problems in plates and shells. In terms of both stress and strain components, the complete Reissner functional for the case wherein displacements are prescribed at the boundaries is simply

$$U'' = \int_V \{\sigma_x \epsilon_x + \sigma_y \epsilon_y + \tau_{xy}\gamma_{xy} + \tau_{xz}\gamma_{xz} + \tau_{yz}\gamma_{yz} - F'\}dV \qquad (1)$$

where F' is the complementary energy density for a nonlinear elastic material and may be shown to be given by

$$F' = \int_0^{\sigma_{eff}} \epsilon_{eff} d\sigma_{eff}$$

The relation between effective stress σ_{eff} and effective strain ϵ_{eff} relative to the uniaxial stress-strain curve for the material may be expressed in the general form given by the Ramberg-Osgood formula

$$\epsilon_{eff} = \frac{\sigma_{eff}}{E} + K\left(\frac{\sigma_{eff}}{E}\right)^n$$

where K and n are constants which depend on a given material. With these relations, the functional can further be expressed as

$$U'' = \int_V \{\sigma_x \epsilon_x + \sigma_y \epsilon_y + \tau_{xy}\gamma_{xy} + \tau_{xz}\gamma_{xz} + \tau_{yz}\gamma_{yz} - \left[\frac{\sigma_{eff}^2}{2E} + \frac{KE}{n+1}\left(\frac{\sigma_{eff}}{E}\right)^{n+1}\right]\}dV \qquad (2)$$

Next, the coordinates are nondimensionalized by introducing the quantities $\xi = 2mx/L$ and $\eta = 2ny/b$; the total volume is given by $V = 2t_f Lb$. For convenience in computer calculations, the functional is rewritten as

$$\frac{U''}{EV} = \int_0^1\int_0^1 \{\frac{\sigma_x'}{E}\epsilon_x' + \frac{\sigma_y'}{E}\epsilon_y' + \frac{\tau_{xy}'}{E}\gamma_{xy}' + \frac{\sigma_x''}{E}\epsilon_x'' + \frac{\sigma_y''}{E}\epsilon_x'' + \frac{\tau_{xy}''}{E}\gamma_{xy}''$$

$$+ \frac{1}{4}\frac{G_c t_c}{E t_f}(\gamma_{xz}^2 + \gamma_{yz}^2) - \frac{1}{4}[\left(\frac{\sigma_{eff}}{E}\right)_t^2 + \left(\frac{\sigma_{eff}}{E}\right)_b^2] - \frac{K}{2(n+1)}[\left(\frac{\sigma_{eff}}{E}\right)_t^{n+1}$$

$$+ \left(\frac{\sigma_{eff}}{E}\right)_b^{n+1}]\}d\xi d\eta \qquad (3)$$

where from Appendix I,

$$\sigma'_x = \frac{1}{2}[(\sigma_x)_t + (\sigma_x)_b]$$

$$\epsilon'_x = u_{,x} + \frac{1}{2} w^2_{,x}$$

$$\sigma'_y = \frac{1}{2}[(\sigma_y)_t + (\sigma_y)_b]$$

$$\epsilon'_y = v_{,y} + \frac{1}{2} w^2_{,y}$$

$$\tau'_{xy} = \frac{1}{2}[(\tau_{xy})_t + (\tau_{xy})_b]$$

$$\gamma'_{xy} = u_{,y} + v_{,x} + w_{,x} w_{,y}$$

$$\sigma''_x = \frac{1}{2}[(\sigma_x)_t - (\sigma_x)_b]$$

$$\epsilon''_x = \frac{h}{2}(w_{,xx} - \gamma_{xz,x})$$

$$\sigma''_y = \frac{1}{2}[(\sigma_y)_t - (\sigma_y)_b]$$

$$\epsilon''_y = \frac{1}{2}(w_{,yy} - \gamma_{yz,y})$$

$$\tau''_{xy} = \frac{1}{2}[(\tau_{xy})_t - (\tau_{xy})_b]$$

$$\gamma''_{xy} = h[w_{,xy} - \frac{1}{2}(\gamma_{xz,y} + \gamma_{yz,x})]$$

and the functional has been separated into the contributions of the direct and bending stresses and strains in the two faces, and the shear stresses and strains in the core.

The functional given by equation (3) may be utilized in the indirect variational approach to develop the Euler equations and boundary conditions of the problem, and in the direct variational approach (Rayleigh-Ritz procedure) to determine the generalized stress and strain distributions compatible with the geometric boundary conditions stipulated for the problem. The two approaches are utilized in Appendixes I and II, respectively.

METHOD OF SOLUTION

ELASTIC SOLUTION

In the elastic case, the functional (equation (3)) may be written as

$$U'' = \int_0^L \int_0^b \{N_x(u_{,x} + \frac{1}{2}w_{,x}^2) + N_y(v_{,y} + \frac{1}{2}w_{,y}^2) + N_{xy}(u_{,y} + v_{,x} + w_{,x}w_{,y})$$
$$- M_x(w_{,xx} - \gamma_{xz,x}) - M_y(w_{,yy} - \gamma_{yz,x})$$
$$+ 2M_{xy}[w_{,xy} - \frac{1}{2}(\gamma_{xz,y} + \gamma_{yz,x})] - \frac{1}{4Et_f}[N_x^2 + N_y^2 - N_xN_y + 3N_{xy}^2]$$
$$- \frac{1}{Et_fh^2}[M_x^2 + M_y^2 - M_xM_y + 3M_{xy}^2] + \frac{1}{2}G_ct_c(\gamma_{xz}^2 + \gamma_{yz}^2)\}dxdy \qquad (4)$$

With the forcing function taken as the unit shortening, $\bar{u}$, the generalized displacements and forces satisfying at least geometric boundary conditions (see Appendix I) are assumed to be

$$u = \bar{u}x$$
$$v = 0$$
$$w = \bar{C} \sin \frac{m\pi x}{L} \sin \frac{n\pi y}{b}$$
$$\gamma_{xz} = \bar{D} \cos \frac{m\pi x}{L} \sin \frac{n\pi y}{b}$$
$$\gamma_{yz} = \bar{E} \sin \frac{m\pi x}{L} \cos \frac{n\pi y}{b} \qquad (5)$$
$$N_x = \bar{F} \cos \frac{2n\pi y}{b} + N_{xo}$$
$$N_y = \bar{G} \cos \frac{2m\pi x}{L}$$
$$N_{xy} = 0$$
$$M_x = \bar{I} \sin \frac{m\pi x}{L} \sin \frac{n\pi y}{b}$$

$$M_y = \bar{J} \sin \frac{m\pi x}{L} \sin \frac{n\pi y}{b}$$

$$M_{xy} = \bar{K} \cos \frac{m\pi x}{L} \cos \frac{n\pi y}{b}$$

where $\bar{C}$, $\bar{D}$, $\bar{E}$, $\bar{F}$, $\bar{G}$, $\bar{I}$, $\bar{J}$ and $\bar{K}$ are arbitrary coefficients whose magnitudes are to be determined from application of the variational principle. Substitution of the assumed functions into the functional (equation (4)) and subsequent integration over the given limits yields a function independent of x and y. Application of Reissner's principle (variation with respect to both assumed stress and strain states) yields 9 simultaneous equations from which the 9 coefficients can be determined explicity in terms of the applied unit shortening. A detailed development is given in Appendix II. With the coefficients established for any given value of unit shortening, the stresses and strains at each point of the plate and, thus, the stress distribution are known. The average stress or load per unit length at any cross section of the plate may be plotted versus end shortening to produce the load-shortening curve in the elastic postbuckling range. Typical load distributions (nondimensionalized with respect to the critical load $(N_{xo})_{cr}$) for several values of the applied shortening parameter $\bar{u}$ (nondimensionalized with respect to the critical shortening $\bar{u}_{cr}$) are shown in Figure 3. The average load ratio $(N_x)_{av}/(N_x)_{cr}$ is plotted against $\bar{u}/\bar{u}_{cr}$ in Figure 4. For $\gamma = 0$ (infinite shear rigidity in core), the results shown in Figure 4 are identical with the elastic-solution results obtained in References 1 through 3 for square or infinitely long plates. The reduction in load-carrying capability for $\gamma = 0.25$, 0.5, and 1.0 is vividly portrayed in Figure 4. It should be noted that the load-shortening curves appear as straight lines only because a one-term approximation has been utilized to represent the buckled shape. In reality, this one-term approximation is exact at buckling and less and less accurate as $\bar{u}/\bar{u}_{cr}$ increases. As shown in References 1 through 3, for example, the straight-line approximation to the load-shortening curve for square or infinitely long plates overestimates the exact average stress by only about 10 percent when $\bar{u}/\bar{u}_{cr}$ is as great as 9. Since the large-deflection plate theory is being utilized, the lateral deflection of the plate can be determined. The effect of transverse shear on maximum deflection is shown in Figure 5.

PLASTIC SOLUTION

In the plastic range, K is not zero; therefore, the exponential terms will appear in the functional. This makes it impossible to apply the variational principle to obtain an analytic solution for the 9 coefficients. However, the variation can be carried out numerically. For a certain value of unit shortening, approximate numerical values of the coefficients may be obtained by taking the numerical value of the coefficients of the elastic solution as initial trial values for the Newton-Raphson iteration method in the plastic solution. When the differences between the elastic solution and plastic solution values of the corresponding coefficients become large,

the coefficient values of the preceding plastic solution point may be used as initial values for the following point. The principal steps are detailed in Appendix III. After the approximate values of the 9 coefficients are found for an assigned value of unit shortening, then, using the same process as in the elastic case, the stresses and strains at each point, as well as the total energy, can be calculated. Stress distributions, average stresses, and load-shortening curves follow directly. Load-shortening curves for plates 1 and 4, with $\gamma = 0$, 0.25, and 0.5 and plasticity effects included, are shown in Figures 6 and 7.

RESULTS AND DISCUSSION

The main objective of this report is to establish the effect of transverse shear flexibility on the postbuckling load-carrying ability of both elastic and inelastic plates. As can be seen from Figures 3 and 4, based upon the all-elastic analysis, both the load (stress) distribution across the plate and the average load are markedly changed by transverse shear effects. In fact, the slope of the load-shortening curve of the rigid core is reduced from 1/2 (the classical result for conventional plates with straight unloaded edges) by more than 20 percent as soon as γ reaches the value of 1/3. Nevertheless, Figure 4 indicates that a substantial load-carrying capacity exists in the elastic sandwich plate. Now, from the results of the inelastic solution (Figure 6 and 7), it can be seen that plasticity affects a rigid-core plate to a much greater extent than it does a plate with finite shear flexibility in the core. In other words, at the same end-shortening ratio, the effective strain levels in the conventional plate are sufficiently high to reduce the stresses and, hence, the average stress, such that the postbuckling-range load ratio is much the same for a conventional ($\gamma = 0$) and sandwich plate ($\gamma = 0.25, 0.5$). The results shown in Figures 6 and 7 indicate that the usual load-carrying capability associated with conventional plates in the well-developed inelastic postbuckled range is not too greatly affected by the presence of transverse shear in the case of the postbuckled sandwich plate.

In this investigation, considerations of the face-wrinkling (Reference 5) and face-dimpling (honeycomb sandwich only) instability modes have been neglected. At the same time, both waveform changes and buckle wavelength changes during postbuckling have been neglected (see Reference 3). The effects considered in Reference 3 reduce postbuckling strength and cause the occurrence of well-defined maximum loads. Thus, it appears from the results presented herein that there is some justification for designing sandwich plate structures for the postbuckling range, since the plasticity and waveform-wavelength change phenomena (Reference 3) reduce load-carrying capacity (maximum strength) to a greater extent than does transverse shear. Of course, in any design exercise, the other modes of initial buckling must be considered.

CONCLUDING REMARKS

An investigation of the postbuckling behavior of sandwich plates loaded into the plastic range has been undertaken. In the absence of inelastic behavior, it is demonstrated that transverse shear effects significantly reduce the load-carrying capability. However, when inelastic deformations are taken into account, the load-carrying capability becomes almost independent of the transverse shear flexibility of the sandwich core. This result indicates that, barring initial buckling in other than the general instability mode, the main effect of transverse shear on the postbuckling load-carrying capability of a plate is to precipitate failure (maximum strength) at a lower value of end shortening, with little change in the ratio of maximum to buckling load. Future work should be directed toward establishing the magnitude and effect of inelastic effects in the core on the maximum strength of plates.

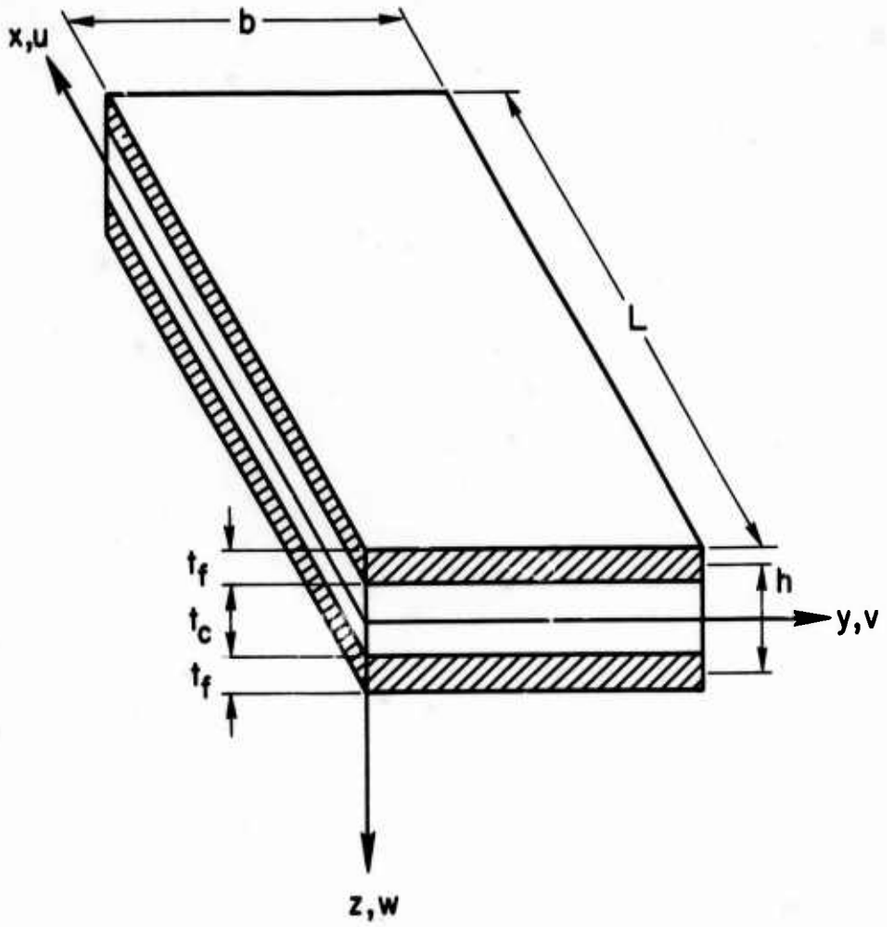

Figure 1. Plate Geometry and Coordinate System.

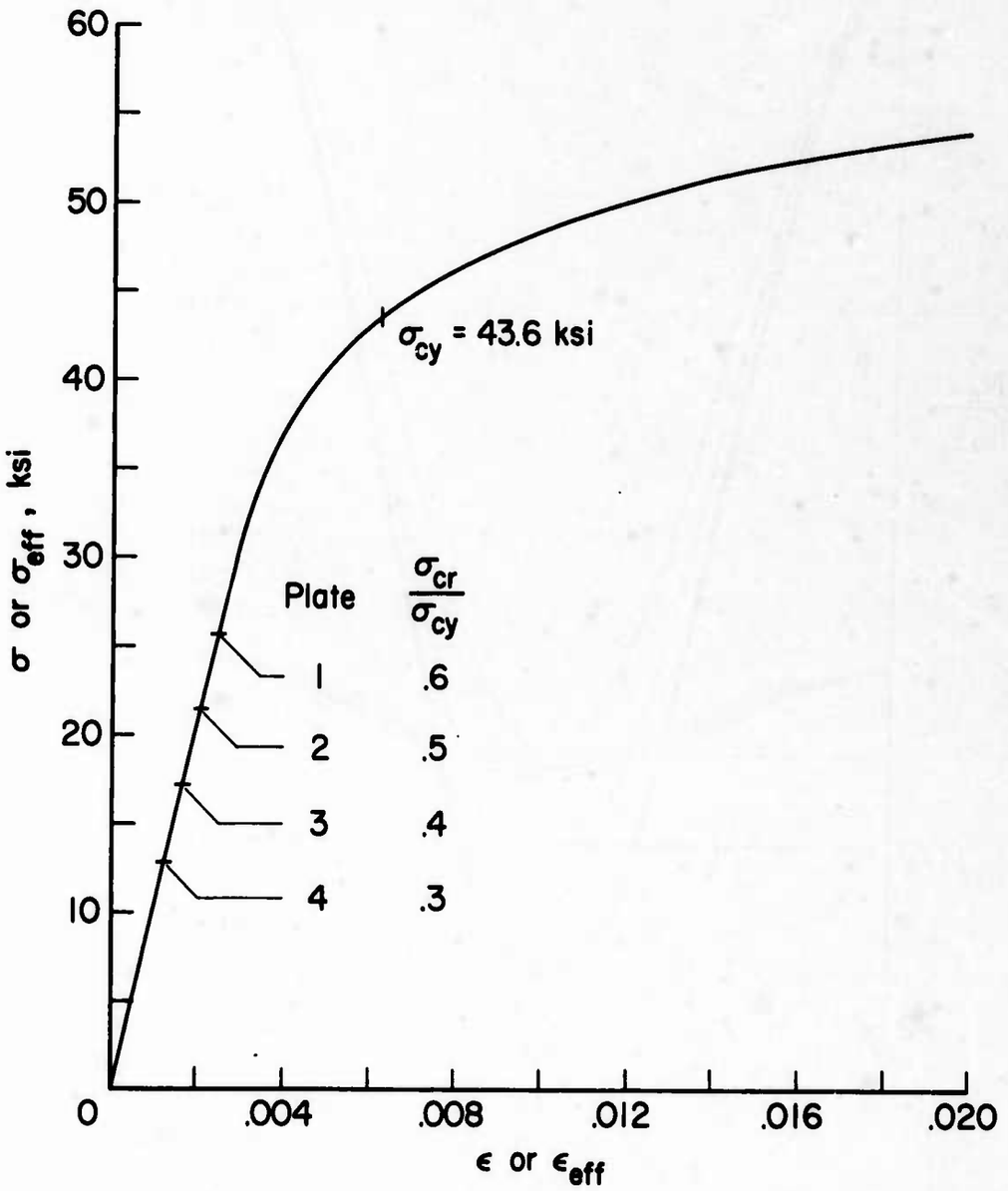

Figure 2. Compressive Stress-Strain Curve and Initial Buckling Stresses for 2024-T3 Aluminum-Alloy Plates Analyzed. (From Reference 1, Figure 2.)

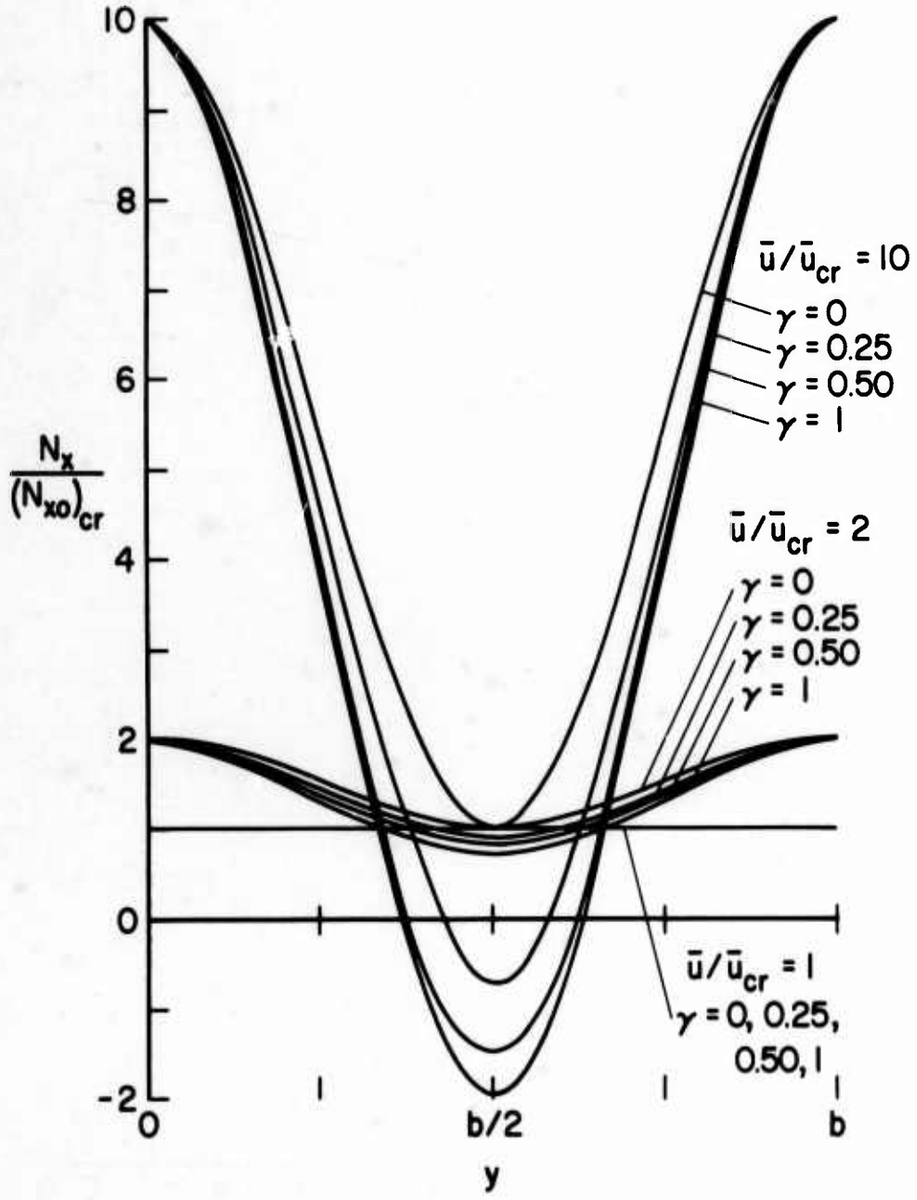

Figure 3. Variation of $N_x/(N_{xo})_{cr}$ Across Plate at Any Cross Section.

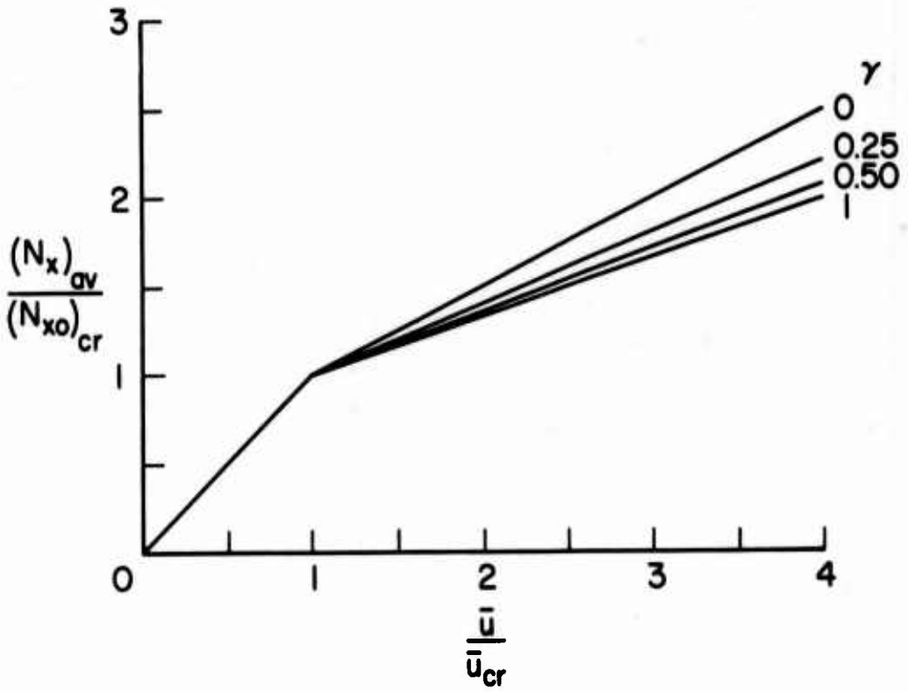

Figure 4. Variation of $(N_x)_{av}/(N_{xo})_{cr}$ with $\bar{u}/\bar{u}_{cr}$ for Several Values of the Transverse Shear Stiffness Parameter γ.

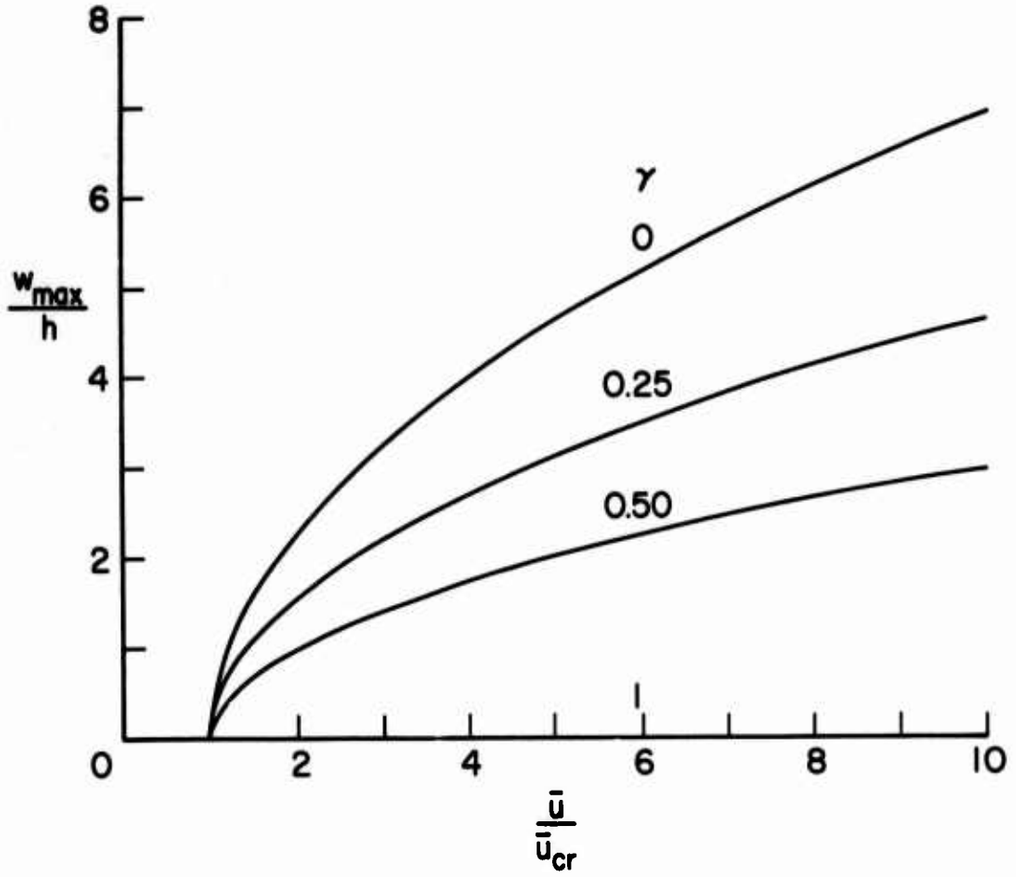

Figure 5. Variation of w_{max}/h With $\bar{u}/\bar{u}_{cr}$ for Several Values of the Transverse Shear Stiffness Parameter γ.

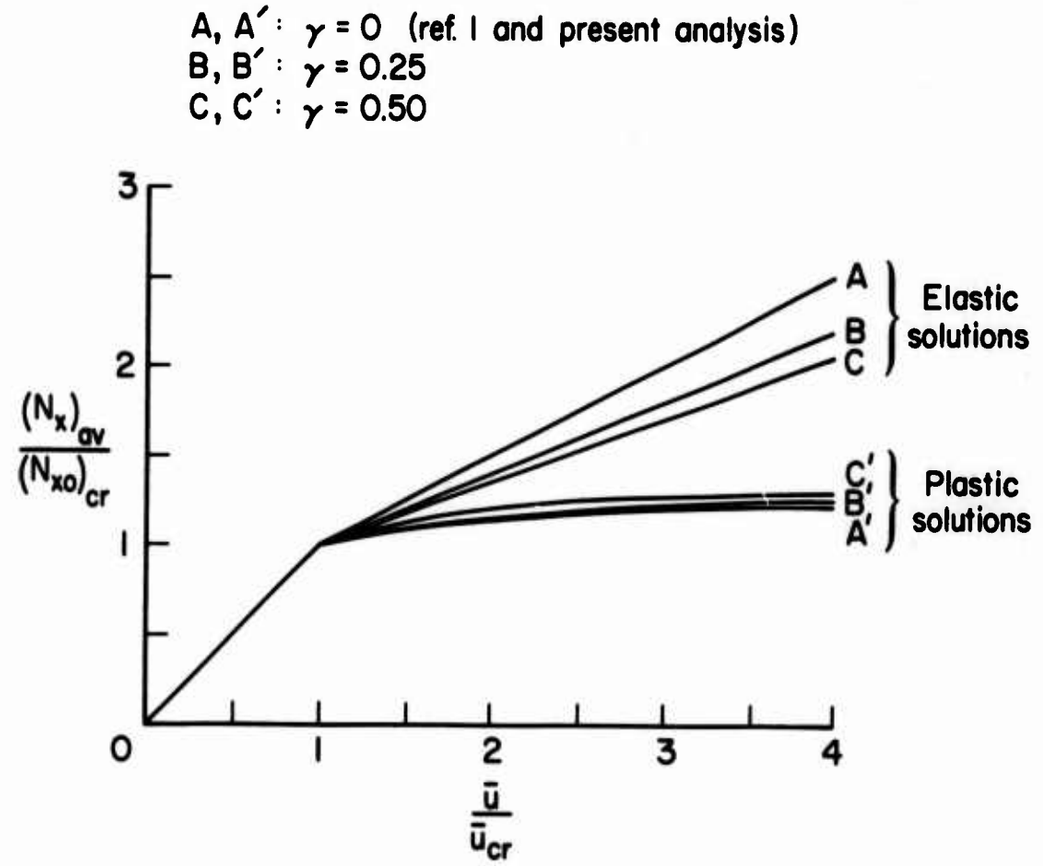

Figure 6. Variation of $(N_x)_{av}/(N_{xo})_{cr}$ With $\bar{u}/\bar{u}_{cr}$, Plate 1, σ_{cr}/σ_{cy} = 0.6.

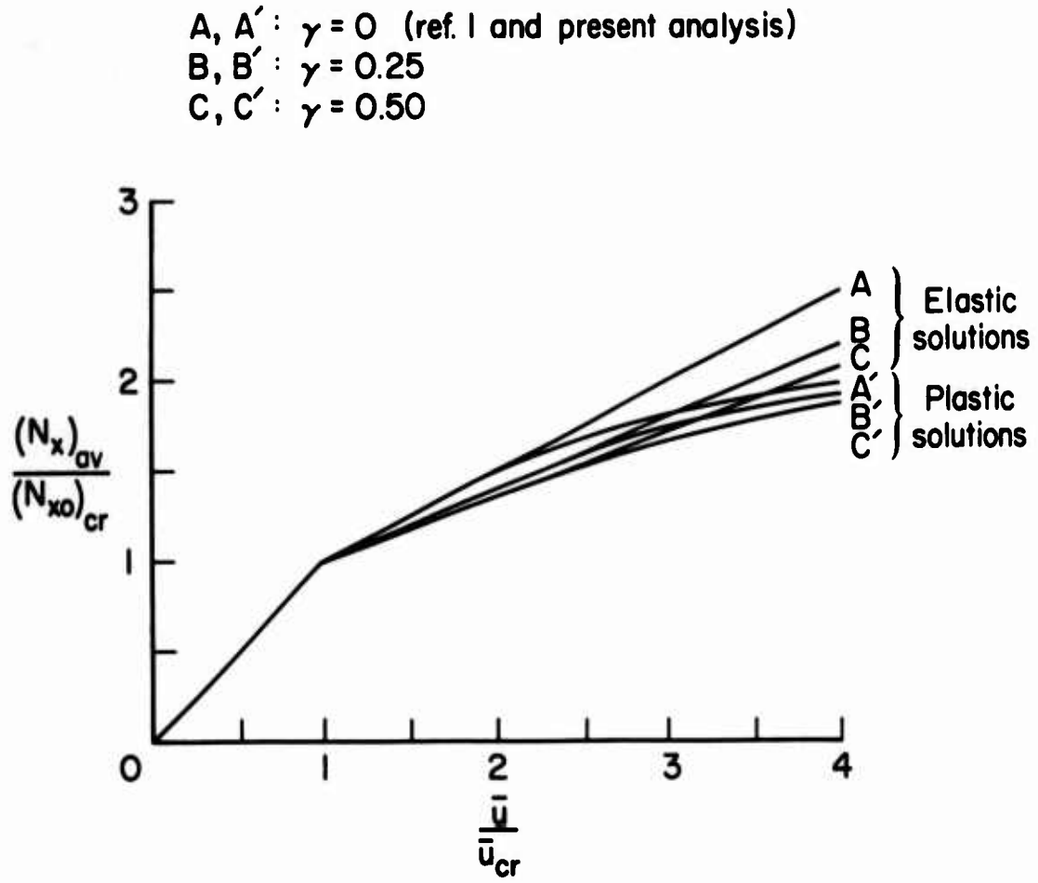

Figure 7. Variation of $(N_x)_{av}/(N_{xo})_{cr}$ with $\bar{u}/\bar{u}_{cr}$, Plate 4, σ_{cr}/σ_{cy} = 0.3.

LITERATURE CITED

1. Mayers, J.,and Budiansky, B., ANALYSIS OF BEHAVIOR OF SIMPLY SUPPORTED FLAT PLATES COMPRESSED BEYOND BUCKLING INTO THE PLASTIC RANGE, NACA Technical Note 3368, 1955.

2. Mayers, J., Nelson, E., and Smith, L. B., MAXIMUM STRENGTH ANALYSIS OF POSTBUCKLED RECTANGULAR PLATES, Stanford University Department of Aeronautics and Astronautics; SUDAAR 215, 1964.

3. Mayers, J.,and Nelson, E., ELASTIC AND MAXIMUM STRENGTH ANALYSIS OF POSTBUCKLED RETANGULAR PLATES BASED UPON MODIFIED VERSIONS OF REISSNER'S VARIATIONAL PRINCIPLE, Stanford University Department of Aeronautics and Astronautics; SUDAAR 262, 1966. (Also, preprint No. 68-171, AIAA 6th Aerospace Sciences Meeting, New York, January 1968.)

4. Stein, M.,and Mayers, J., A SMALL-DEFLECTION THEORY FOR CURVED SANDWICH PLATES; NACA TR 1008, 1951.

5. Benson, A. S.,and Mayers, J., GENERAL INSTABILITY AND FACE WRINKLING OF SANDWICH PLATES – UNIFIED THEORY AND APPLICATIONS, AIAA Journal, Vol. 5, No. 4, April 1967, pp. 729-739.

6. Bartelds, G.,and Mayers, J., UNIFIED THEORY FOR THE BENDING AND BUCKLING OF SANDWICH SHELLS – APPLICATION TO AXIALLY COMPRESSED CIRCULAR CYLINDRICAL SHELLS, Proceedings of the AIAA/ASME 8th Structures, Structural Dynamics and Materials Conference, Palm Springs, Calif., March 1967, pp. 619-637.

7. Mayers, J.,and Rehfield, L. W., FURTHER NONLINEAR CONSIDERATIONS IN THE POSTBUCKLING OF AXIALLY-COMPRESSED CIRCULAR CYLINDRICAL SHELLS, Development in Mechanics, Volume 3, The Proceedings of the Ninth Midwestern Mechanics Conference, Part I, Solid Mechanics and Materials, John Wiley and Sons, Inc., New York, 1967, pp. 145-160.

APPENDIX I

EULER EQUATIONS AND BOUNDARY CONDITIONS DERIVED FROM THE VARIATIONAL PRINCIPLE

1. REISSNER FUNCTIONAL

For a sandwich plate as shown in Figure 1, the Reissner functionals are

$$U''_{t,b} = \int_V \{(\sigma_x \epsilon_x)_{t,b} + (\sigma_y \epsilon_y)_{t,b} + (\tau_{xy}\gamma_{xy})_{t,b} - F'_{t,b}\}dV$$

for the face plates and

$$U''_c = \int_V \{\tau_{xz}\gamma_{xz} + \tau_{yz}\gamma_{yz} - F'_c\}dV$$

for the core. The total functional is given by

$$U'' = U''_t + U''_b + U''_c$$

The strain-displacement relations for small strain, moderate-rotation plate theory, with transverse shear effects included (see Reference 7), become

$$(\epsilon_x)_{t,b} = u_{,x} + \frac{1}{2} w^2_{,x} \pm \frac{h}{2}(w_{,xx} - \gamma_{xz,x})$$

$$(\epsilon_y)_{t,b} = v_{,y} + \frac{1}{2} w^2_{,y} \pm \frac{h}{2}(w_{,yy} - \gamma_{yz,y})$$

$$(\gamma_{xy})_{t,b} = u_{,y} + v_{,x} + w_{,x}w_{,y} \pm h[w_{xy} - \frac{1}{2}(\gamma_{xz,y} + \gamma_{yz,x})]$$

where the + and - signs correspond to the top and bottom faces, respectively.

The complementary energy density in the facings and core, respectively, is

$$F'_{t,b} = \frac{1}{2E}[(\sigma_x)^2_{t,b} + (\sigma_y)^2_{t,b} - (\sigma_x\sigma_y)^2_{t,b} + 3(\tau_{xy})^2_{t,b}]$$

$$F'_c = \frac{1}{2G_c}[\tau^2_{xz} + \tau^2_{yz}]$$

With these relations, the functional in the elastic case becomes

$$
\begin{aligned}
U'' = \int_V \{ & (\sigma_x)_t [u_{,x} + \tfrac{1}{2} w_{,x}^2 + \tfrac{h}{2}(w_{,xx} - \gamma_{xz,x})] \\
& + (\sigma_x)_b [u_{,x} + \tfrac{1}{2} w_{,x}^2 - \tfrac{h}{2}(w_{,xx} - \gamma_{xz,x})] \\
& + (\sigma_y)_t [v_{,y} + \tfrac{1}{2} w_{,y}^2 + \tfrac{h}{2}(w_{,yy} - \gamma_{yz,y})] \\
& + (\sigma_y)_b [v_{,y} + \tfrac{1}{2} w_{,y}^2 - \tfrac{h}{2}(w_{,yy} - \gamma_{yz,y})] \\
& + (\tau_{xy})_t [u_{,y} + v_{,x} + w_{,x} w_{,y} + h(w_{,xy} - \tfrac{1}{2}(\gamma_{xz,y} + \gamma_{yz,x}))] \\
& + (\tau_{xy})_b [u_{,y} + v_{,x} + w_{,x} w_{,y} - h(w_{,xy} - \tfrac{1}{2}(\gamma_{xz,y} + \gamma_{yz,x}))] \\
& - \tfrac{1}{2E}[(\sigma_x)_t^2 + (\sigma_y)_t^2 - (\sigma_x)_t(\sigma_y)_t + 3(\tau_{xy})_t^2 \\
& + (\sigma_x)_b^2 + (\sigma_y)_b^2 - (\sigma_x)_b(\sigma_y)_b + 3(\tau_{xy})_b^2] \\
& + \tau_{xz}\gamma_{xz} + \tau_{yz}\gamma_{yz} - \tfrac{1}{2G}(\tau_{xz}^2 + \tau_{yz}^2)\} dV
\end{aligned}
\tag{6a}
$$

Introduction of the average stresses and bending moments

$$\sigma'_x = \tfrac{1}{2}[(\sigma_x)_t + (\sigma_x)_b]$$

$$\sigma'_y = \tfrac{1}{2}[(\sigma_y)_t + (\sigma_y)_b]$$

$$\tau'_{xy} = \tfrac{1}{2}[(\tau_{xy})_t + (\tau_{xy})_b]$$

$$M_x = -t_f \tfrac{h}{2}[(\sigma_x)_t - (\sigma_x)_b]$$

$$M_y = -t_f \tfrac{h}{2}[(\sigma_y)_t - (\sigma_y)_b]$$

$$M_{xy} = t_f \tfrac{h}{2}[(\tau_{xy})_t - (\tau_{xy})_b]$$

into equation (6a) yields

$$U'' = t_f \int_0^L \int_0^b [(\sigma_x)_t + (\sigma_x)_b](u_{,x} + \tfrac{1}{2} w_{,x}^2) + [(\sigma_x)_t - (\sigma_x)_b] \tfrac{h}{2}(w_{,xx} - \gamma_{xz,x})$$

$$+ [(\sigma_y)_t + (\sigma_y)_b](v_{,y} + \tfrac{1}{2} w_{,y}^2) + [(\sigma_y)_t - (\sigma_y)_b]\tfrac{h}{2}(w_{,yy} - \gamma_{yz,y})$$

$$+ [(\tau_{xy})_t + (\tau_{xy})_b](u_{,y} + v_{,x} + w_{,x} w_{,y})$$

$$+ [(\tau_{xy})_t - (\tau_{xy})_b]h(w_{,xy} - \tfrac{1}{2}[\gamma_{xz,y} + \gamma_{yz,x}])$$

$$- \frac{1}{2E}[(\sigma_x)_t^2 + (\sigma_y)_t^2 - (\sigma_x)_t(\sigma_y)_t + 3(\tau_{xy})_t^2$$

$$+ (\sigma_x)_b^2 + (\sigma_y)_b^2 - (\sigma_x)_b(\sigma_y)_b + 3(\tau_{xy})_b^2]$$

$$+ \frac{t_c}{t_f}[\tau_{xz}\gamma_{xz} - \tau_{yz}\gamma_{yz} - \frac{1}{2G_c}(\tau_{xz}^2 + \tau_{yz}^2)]dxdy \qquad (6b)$$

or, in terms of local average stresses and moments,

$$U'' = t_f \int_0^L \int_0^b \{2\sigma'_x(u_{,x} + \tfrac{1}{2} w_{,x}^2) + 2\sigma'_y(v_{,y} + \tfrac{1}{2} w_{,y}^2) + 2\tau'_{xy}(u_{,y} + v_{,x}$$

$$+ w_{,x} w_{,y}) - \frac{M_x}{t_f}(w_{,xx} + \gamma_{xz,x}) - \frac{M_y}{t_f}(w_{,yy} - \gamma_{yz,y})$$

$$+ 2\frac{M_{xy}}{t_f}[w_{,xy} - \tfrac{1}{2}(\gamma_{xz,y} + \gamma_{yz,x})] - \frac{1}{E}[\sigma'^2_x + \sigma'^2_y - \sigma'_x\sigma'_y + 3\tau'^2_{xy}$$

$$+ \frac{1}{(t_f h)^2}(M_x^2 + M_y^2 - M_x M_y + 3M_{xy}^2)]$$

$$+ \frac{t_c}{t_f}[\tau_{xz}\gamma_{xz} + \tau_{yz}\gamma_{yz} - \frac{1}{2G_c}(\tau_{xz}^2 + \tau_{yz}^2)]\}dxdy \qquad (6c)$$

2. EULER EQUATIONS AND BOUNDARY CONDITIONS

The vanishing of the first variation of equation (6c) with respect to σ'_x, σ'_y, τ'_{xy}, M'_x, M'_y, M'_{xy}, u, v, w, γ_{xz} and γ_{yz} gives

$$\delta U'' = t_f \int_0^L \int_0^b \{2\delta\sigma'_x(u_{,x} + \tfrac{1}{2} w_{,x}^2) + 2\sigma'_x(\delta u_{,x} + w_{,x}\delta w_{,x})$$

$$+ 2\delta\sigma'_y(v_{,y} + \tfrac{1}{2} w_{,y}^2) + 2\sigma'_y(\delta v_{,y} + w_{,y}\delta w_{,y})$$

$$+ 2\delta\tau'_{xy}(u_{,y} + v_{,x} + w_{,x}w_{,y}) + 2\tau'_{xy}(\delta u_{,y} + \delta v_{,x} + w_{,y}\delta w_{,x} + w_{,x}\delta w_{,y})$$

$$- \frac{\delta M_x}{t_f}(w_{,xx} - \gamma_{xz,x}) - \frac{M_x}{t_f}(\delta w_{,xx} - \delta\gamma_{xz,x})$$

$$- \frac{\delta M_y}{t_f}(w_{,yy} - \gamma_{yz,y}) - \frac{M_y}{t_f}(\delta w_{,yy} - \delta\gamma_{yz,y})$$

$$+ 2\frac{\delta M_{xy}}{t_f}[w_{,xy} - \tfrac{1}{2}(\gamma_{xz,y} + \gamma_{yz,x})] + 2\frac{M_{xy}}{t_f}[\delta w_{,xy} - \tfrac{1}{2}(\delta\gamma_{xz,y} + \delta\gamma_{yz,x})]$$

$$-2[\frac{\partial F'}{\partial \sigma'_x}\delta\sigma'_x + \frac{\partial F'}{\partial \sigma'_y}\delta\sigma'_y + \frac{\partial F'}{\partial \tau'_{xy}}\delta\tau'_{xy} + \frac{\partial F'}{\partial M_x}\delta M_x + \frac{\partial F'}{\partial M_y}\delta M_y + \frac{\partial F'}{\partial M_{xy}}\delta M_{xy}]$$

$$+ \frac{t_c}{t_f}[\delta\tau_{xy}\gamma_{xz} + \tau_{xy}\delta\gamma_{xz} + \delta\tau_{yz}\gamma_{yz} + \tau_{yz}\delta\gamma_{yz} - \frac{1}{G_c}(\tau_{xz}\delta\tau_{xz} + \tau_{yz}\delta\tau_{yz})]\}dxdy = 0 \tag{7}$$

After integration by parts and regrouping of terms, equation (7) becomes

$$\delta U'' = 2t_f \int_0^L \int_0^b \{(u_{,x} + \tfrac{1}{2}w_{,x}^2 - \frac{\partial F'}{\partial \sigma'_x})\delta\sigma'_x + (v_{,y} + \tfrac{1}{2}w_{,y}^2 - \frac{\partial F'}{\partial \sigma'_y})\delta\sigma'_y$$

$$+ (u_{,y} + v_{,x} + w_{,x}w_{,y} - \frac{\partial F'}{\partial \tau'_{xy}})\delta\tau'_{xy}$$

$$- (\frac{w_{,xx}}{2t_f} - \frac{\gamma_{xz,x}}{2t_f} + \frac{\partial F'}{\partial M_x})\delta M_x - (\frac{w_{,yy}}{2t_f} - \frac{\gamma_{yz,y}}{2t_f} + \frac{\partial F'}{\partial M_y})\delta M_y$$

$$+ [\frac{w_{,xy}}{t_f} - \frac{1}{2t_f}(\gamma_{xz,y} + \gamma_{yz,x}) - \frac{\partial F'}{\partial M_{xy}}]\delta M_{xy}$$

(continued)

$$+\frac{t_c}{2t_f}(\gamma_{xz}-\frac{\tau_{xz}}{G_c})\delta\tau_{xy}+\frac{t_c}{2t_f}(\gamma_{yz}-\frac{\tau_{yz}}{G_c})\delta\tau_{yz}$$

$$-(\sigma'_{x,x}+\tau'_{xy,y})\delta u-(\sigma'_{y,y}+\tau'_{xy,x})\delta v$$

$$-[(\sigma'_x w_{,x})_{,x}+(\sigma'_y w_{,y})_{,y}+(\tau_{xy} w_{,y})_{,x}+(\tau'_{xy} w_{,x})_{,y}$$

$$+\frac{1}{2t_f}(M_{x,xx}+M_{y,yy}-2M_{xy,xy})]\delta w+\frac{1}{2t_f}[-M_{y,y}+M_{xy,x}+t_c\tau_{yz}]\delta\gamma_{yz}$$

$$+\frac{1}{2t_f}[-M_{x,x}+M_{xy,y}+t_c\tau_{xz}]\delta\gamma_{xz}\}dxdy$$

$$+2t_f\int_0^b\{\sigma'_x\delta u|_0^L\}dy+2t_f\int_0^L\{\tau'_{xy}\delta u|_0^b\}dx$$

$$+2t_f\int_0^L\{\sigma'_y\delta u|_0^b\}dx+2t_f\int_0^b\{\tau'_{xy}\delta v|_0^L\}dy$$

$$+\int_0^b\{[2t_f\sigma'_x w_{,x}+2t_f\tau'_{xy} w_{,y}+M_{x,x}-M_{xy,y}]\delta_w|_0^L\}dy$$

$$+\int_0^L\{[2t_f\sigma'_y w_{,y}+2t_f\tau'_{xy} w_{,x}+M_{y,y}-M_{xy,x}]\delta w|_0^b\}dx$$

$$+\int_0^b\{M_x\delta\gamma_{xz}|_0^L\}dy-\int_0^L\{M_{xy}\delta\gamma_{xz}|_0^b\}dx$$

$$+\int_0^L\{My\delta\gamma_{yz}|_0^b\}dx-\int_0^b\{M_{xy}\delta\gamma_{yz}|_0^L\}dy$$

$$-\int_0^b\{M_x\delta w_{,x}|_0^L\}dy+\int_0^L\{M_{xy}\delta w_{,x}|_0^b\}dx$$

(continued)

$$-\int_0^L \{M_y \delta w_{,y}\Big|_0^b\}dx + \int_0^b \{M_{xy} \delta w_{,y}\Big|_0^L\}dy = 0 \tag{8}$$

For the above expression to vanish for arbitrary states of stress and displacement consistent with the geometric boundary conditions, each of the terms must vanish identically. These terms lead to the Euler equations and natural boundary conditions as follows:

Stress-displacement relations:

$$\left.\begin{aligned} u_{,x} + \frac{1}{2} w_{,x}^2 - \frac{\partial F'}{\partial \sigma'_x} &= 0 \\ v_{,y} + \frac{1}{2} w_{,y}^2 - \frac{\partial F'}{\partial \sigma'_y} &= 0 \\ u_{,y} + v_{,x} + w_{,x} w_{,y} - \frac{\partial F'}{\partial \tau'_{xy}} &= 0 \end{aligned}\right\} \tag{9}$$

Moment-curvature relations:

$$\left.\begin{aligned} \frac{1}{2t_f}(w_{,xx} - \gamma_{xz,x}) + \frac{\partial F'}{\partial M_x} &= 0 \\ \frac{1}{2t_f}(w_{,yy} - \gamma_{yz,y}) + \frac{\partial F'}{\partial M_y} &= 0 \\ \frac{1}{t_f}[w_{,xy} - \frac{1}{2}(\gamma_{xz,y} + \gamma_{yz,x})] - \frac{\partial F'}{\partial M_{xy}} &= 0 \end{aligned}\right\} \tag{10}$$

Shear stress-shear strain relations:

$$\left.\begin{aligned} \frac{t_c}{2t_f}(\gamma_{xz} - \frac{\tau_{xz}}{G_c}) &= 0 \\ \frac{t_c}{2t_f}(\gamma_{yz} - \frac{\tau_{yz}}{G_c}) &= 0 \end{aligned}\right\} \tag{11}$$

Inplane equilibrium equations:

$$\left.\begin{aligned} \sigma'_{x,x} + \tau'_{xy,y} &= 0 \\ \sigma'_{y,y} + \tau'_{xy,x} &= 0 \end{aligned}\right\} \tag{12}$$

Out-of-plane equilibrium equation:

$$\sigma'_x w_{,xx} + 2\tau'_{xy} w_{,xy} + \sigma'_y w_{,yy} + \frac{1}{2t_f}(M_{x,xx} - 2M_{xy,xy} + M_{y,yy}) = 0 \qquad (13)$$

Core shear equilibrium equations:

$$\left.\begin{aligned} -M_{x,x} + M_{xy,y} + t_c \tau_{xz} &= 0 \\ -M_{y,y} + M_{xy,x} + t_c \tau_{yz} &= 0 \end{aligned}\right\} \qquad (14)$$

Stress (natural) boundary conditions:

$$\left.\begin{aligned} \tau'_{xy} &= 0 \quad \text{at} \quad y = 0, \quad y = b \\ M_x &= 0 \quad \text{at} \quad x = 0, \quad x = L \\ M_y &= 0 \quad \text{at} \quad y = 0, \quad y = b \end{aligned}\right\} \qquad (15)$$

The geometric boundary conditions that have been enforced are

$$\left.\begin{aligned} w &= 0 \quad \text{at} \quad x = 0, \quad x = L \\ w &= 0 \quad \text{at} \quad y = 0, \quad y = b \\ u &= 0 \quad \text{at} \quad x = 0 \\ u &= \bar{u}L \quad \text{at} \quad x = L \\ v &= 0 \quad \text{at} \quad x = 0, \quad x = L \\ v &= 0 \quad \text{at} \quad y = 0, \quad y = b \end{aligned}\right\} \qquad (16)$$

APPENDIX II

ELASTIC ANALYSIS

1. DIRECT VARIATIONAL METHOD

Substitution of the assumed trigonometric functions given by equation (5) into the functional (equation (4)) and use of the following integrations

$$\int_0^b \cos\left(\frac{2n\pi y}{b}\right)dy = 0$$

$$\int_0^b \cos\left(\frac{2n\pi y}{b}\right)\sin^2\left(\frac{n\pi y}{b}\right)dy = -\frac{b}{4}$$

$$\int_0^b \cos^2\left(\frac{n\pi y}{b}\right)dy = \frac{b}{2}$$

$$\int_0^b \sin^2\left(\frac{n\pi y}{b}\right)dy = \frac{b}{2}$$

$$\int_0^b \cos^2\left(\frac{2n\pi y}{b}\right)dy = \frac{b}{2}$$

as well as corresponding integrations with respect to x, yields

$$\begin{aligned} U'' = {} & Lb\bar{u}N_{xo} - \frac{\pi^2}{16}\frac{m^2b}{L}\bar{C}^2\bar{F} + \frac{\pi^2}{8}\frac{m^2b}{L}\bar{C}^2N_{xo} - \frac{\pi^2}{16}\frac{n^2L}{b}\bar{C}^2\bar{G} \\ & + \frac{\pi^2}{4}\frac{m^2b}{L}\bar{I}\,\bar{C} - \frac{\pi}{4}mb\bar{I}\,\bar{D} + \frac{\pi^2}{4}\frac{n^2L}{b}\bar{J}\,\bar{C} - \frac{\pi}{4}nL\bar{J}\,\bar{E} \\ & + \frac{\pi^2}{2}mn\bar{K}\,\bar{C} - \frac{\pi}{4}nL\bar{K}\,\bar{D} - \frac{\pi}{4}mb\bar{K}\,\bar{E} \\ & - \frac{1}{4Et_f}\left[\frac{Lb}{2}\bar{F}^2 + LbN_{xo}^2 + \frac{Lb}{2}\bar{G}^2\right] - \frac{1}{Et_fh^2}\frac{Lb}{4}\left[\bar{I}^2 + \bar{J}^2 - \bar{I}\,\bar{J} + 3\bar{K}^2\right] \\ & + \frac{1}{2}G_ct_c\frac{Lb}{4}\left[\bar{D}^2 + \bar{E}^2\right] \end{aligned} \qquad (17)$$

The variation of U" with respect to the parameters gives

$$\delta_{\bar{C}}U'' = -\frac{\pi^2}{8}\frac{m^2b}{L}\bar{C}\bar{F} + \frac{\pi^2}{4}\frac{m^2b}{L}\bar{C}N_{xo} - \frac{\pi^2}{8}\frac{n^2L}{b}\bar{C}\bar{G}$$

$$+\frac{\pi^2}{4}\frac{m^2b}{L}\bar{I} + \frac{\pi^2}{4}\frac{n^2L}{b}\bar{J} + \frac{\pi^2}{2}mn\bar{K}^2 = 0 \qquad (18a)$$

$$\delta_{\bar{D}}U'' = -\frac{\pi}{4}mb\bar{I} - \frac{\pi}{4}nL\bar{K} + \frac{1}{4}G_c t_c Lb\bar{D} = 0 \qquad (18b)$$

$$\delta_{\bar{E}}U'' = -\frac{\pi}{4}nL\bar{J} - \frac{\pi}{4}mb\bar{K} + \frac{1}{4}G_c t_c Lb\bar{E} = 0 \qquad (18c)$$

$$\delta_{\bar{F}}U'' = -\frac{\pi^2}{16}\frac{m^2b}{L}\bar{C}^2 - \frac{1}{4Et_f}Lb\bar{F} = 0 \qquad (18d)$$

$$\delta_{\bar{G}}U'' = -\frac{\pi^2}{16}\frac{n^2L}{b}\bar{C}^2 - \frac{1}{4Et_f}Lb\bar{G} = 0 \qquad (18e)$$

$$\delta_{\bar{I}}U'' = \frac{\pi^2}{4}\frac{m^2b}{L}\bar{C} - \frac{\pi}{4}mb\bar{D} - \frac{1}{Et_f h^2}\frac{Lb}{4}[2\bar{I} - \bar{J}] = 0 \qquad (18f)$$

$$\delta_{\bar{J}}U'' = \frac{\pi^2}{4}\frac{n^2L}{b}\bar{C} - \frac{\pi}{4}nL\bar{E} - \frac{1}{Et_f h^2}\frac{Lb}{4}[2\bar{J} - \bar{I}] = 0 \qquad (18g)$$

$$\delta_{\bar{K}}U'' = \frac{\pi^2}{2}mn\bar{C} - \frac{\pi}{4}nL\bar{D} - \frac{\pi}{4}mb\bar{E} - \frac{1}{Et_f h^2}\frac{Lb}{4}\cdot 6\bar{K} = 0 \qquad (18h)$$

$$\delta_{N_{xo}}U'' = Lb\bar{u} + \frac{\pi^2}{8}\frac{m^2b}{L}\bar{C}^2 - \frac{Lb}{2Et_f}N_{xo} = 0 \qquad (18i)$$

First, consideration is given to the linear (excluding N_{xo}) part of equation (18a) and equations (18b), (18c), (18f), (18g) and (18h). These 6 equations are linear and homogeneous with respect to the parameters $\bar{C}$, $\bar{D}$, $\bar{E}$, $\bar{I}$, $\bar{J}$ and $\bar{K}$. A nontrivial solution exists only if

$$\begin{vmatrix} \frac{\pi}{4}\frac{m^2b}{L}N_{xo} & 0 & 0 & \frac{\pi^2}{4}\frac{m^2b}{L} & \frac{\pi^2}{4}\frac{n^2L}{b} & \frac{\pi^2}{2}mn \\ 0 & \frac{1}{4}G_ct_cLb & 0 & -\frac{\pi}{4}mb & 0 & -\frac{\pi}{4}nL \\ 0 & 0 & \frac{1}{4}G_ct_cLb & 0 & -\frac{\pi}{4}nL & -\frac{\pi}{4}mb \\ \frac{\pi^2}{4}\frac{m^2b}{L} & -\frac{\pi}{4}mb & 0 & -\frac{1}{Et_fh^2}\frac{Lb}{2} & \frac{1}{Et_fh^2}\frac{Lb}{4} & 0 \\ \frac{\pi^2}{4}\frac{n^2L}{b} & 0 & -\frac{\pi}{4}nL & \frac{1}{Et_fh^2}\frac{Lb}{4} & -\frac{1}{Et_fh^2}\frac{Lb}{2} & 0 \\ \frac{\pi^2}{2}mn & -\frac{\pi}{4}nL & -\frac{\pi}{4}mb & 0 & 0 & -\frac{1}{Et_fh^2}\frac{3Lb}{2} \end{vmatrix} = 0 \quad (19)$$

2. CRITICAL STRESS

With the introduction of the parameters

$$\beta = \frac{mb}{nL}$$

$$D_s = \frac{2Et_fh^2}{3}$$

$$D_Q = G_ct_c$$

$$\gamma = \frac{D_s\pi^2}{D_Qb^2}$$

$$k_x = \frac{N_{xo}b^2}{D_s\pi^2}$$

expansion of the above determinant leads to

$$\frac{n^4D_Q^2}{4D_s}Lb\gamma^2\beta^2\left\{\frac{(\beta^2+1)^2}{\beta^2[1+n^2\gamma(\beta^2+1)]}+\frac{k_x}{n^2}\right\}=0$$

or

$$k_x = - \frac{(\beta^2+1)^2}{\beta^2[1+n^2\gamma(\beta^2+1)]} \tag{20}$$

For the critical value, $n = 1$ and k_x is minimized with respect to β; that is, $dk_x/d\beta = 0$. This gives

$$\beta = \sqrt{\frac{1+\gamma}{1-\gamma}}$$

Substitution of the initial wavelength parameter value into equation (20) gives

$$(k_x)_{cr} = - \frac{4}{(1+\gamma)^2} \tag{21a}$$

If $\gamma = 0$, that is, D_Q approaches infinity, then

$$(k_x)_{cr}\Big|_{\gamma=0} = -4 \tag{21b}$$

The negative sign simply indicates that $\bar{u}$ has been taken positive in tension.

3. STRESS DISTRIBUTION

The values of all arbitrary parameters may be found in terms of $\bar{C}$ as follows: First, from equations (18b), (18c), (18f), (18g) and (18h),

$$\left.\begin{aligned}
\bar{D} &= \frac{\pi n^2\gamma\beta(\beta^2+1)}{b/n} - \frac{1}{[1+n^2\gamma(\beta^2+1)]}\bar{C} \\
\bar{E} &= \frac{\pi n^2\gamma(\beta^2+1)}{b/n} \cdot \frac{1}{[1+n^2\gamma(\beta^2+1)]}\bar{C} \\
\bar{I} &= \frac{D_Q n^2\gamma(2\beta^2+1)}{2[1+n^2\gamma(\beta^2+1)]}\bar{C} \\
\bar{J} &= \frac{D_Q n^2\gamma(\beta^2+2)}{2[1+n^2\gamma(\beta^2+1)]}\bar{C}
\end{aligned}\right\} \tag{22}$$

Second, equations (18d), (18e) and (18i) give

$$\left.\begin{aligned}
\bar{F} &= -\frac{3\pi^2 D_s \beta^2}{8(b/n)^2}\left(\frac{\bar{C}}{h}\right)^2 = -\frac{3}{8} D_Q n^2 \gamma \beta^2 \left(\frac{\bar{C}}{h}\right)^2 \\
\bar{G} &= -\frac{3\pi^2 D_s}{8(b/n)^2}\left(\frac{\bar{C}}{h}\right)^2 = -\frac{3}{8} D_Q n^2 \gamma \left(\frac{\bar{C}}{h}\right)^2 \\
N_{xo} &= \frac{3D_s}{h^2}\bar{u} + \frac{3\pi^2 D_s \beta^2}{8(b/n)^2}\left(\frac{\bar{C}}{h}\right)^2 = \frac{3D_s}{h^2}\bar{u} + \frac{3}{8} D_Q n^2 \gamma \beta^2 \left(\frac{\bar{C}}{h}\right)^2
\end{aligned}\right\} \qquad (23)$$

Substitution of $\bar{F}$, $\bar{G}$, $\bar{I}$, $\bar{J}$ and $\bar{K}$ into equation (18a) then yields

$$\delta_{\bar{C}}U'' = \frac{3}{64}\frac{D_Q^2}{D_s} n^4 \gamma^2 Lb(\beta^4+1)\left(\frac{\bar{C}}{h}\right)^2 \bar{C} + \frac{D_Q^2}{4D_s} n^4 \gamma^2 Lb\beta^2 \left\{\frac{(\beta^2+1)^2}{\beta^2[1+n^2\gamma(\beta^2+1)]} + \frac{k_x}{n^2}\right\} \bar{C} = 0$$

or

$$\frac{3}{16}(\beta^4+1)\left(\frac{\bar{C}}{h}\right)^2 + \beta^2\left\{\frac{(\beta^2+1)^2}{\beta^2[1+n^2\gamma(\beta^2+1)]} + \frac{k_x}{n^2}\right\} = 0 \qquad (24)$$

When $\beta = \sqrt{\frac{1+\gamma}{1-\gamma}}$ and $n = 1$, the critical value for k_x exists and

$$\left(\frac{\bar{C}}{h}\right)^2 = \frac{8(1-\gamma^2)}{3(1+\gamma^2)}[(k_x)_{cr} - k_x]$$

$$= \frac{32(1-\gamma)}{3(1+\gamma^2)(1+\gamma)}\left[\frac{N_{xo}}{(N_{xo})_{cr}} - 1\right] \qquad (25)$$

Here, it should be mentioned that when equation (25) is substituted into the expressions for the parameter coefficients, all β's should take the value of $\sqrt{(1+\gamma)/(1-\gamma)}$ when the plate is long. For finite length plates, integer values of β must be utilized, just as in the case of conventional plates, to find the lowest critical k_x. Thus,

$$N_x = \bar{F}\cos\left(\frac{2n\pi y}{b}\right) + N_{xo}$$

$$= \frac{(1+\gamma)^2}{(1+\gamma^2)}(N_{xo})_{cr}\left[\frac{N_{xo}}{(N_{xo})_{cr}} - 1\right]\cos\left(\frac{2n\pi y}{b}\right) + N_{xo}$$

or

$$\frac{N_x}{N_{xo}} = \frac{(1+\gamma)^2}{(1+\gamma^2)}\left[\frac{N_{xo}}{(N_{xo})_{cr}} - 1\right]\cos\left(\frac{2n\pi y}{b}\right) + \frac{N_{xo}}{(N_{xo})_{cr}} \tag{26}$$

To find the relation between $\bar{u}$ and N_x, N_{xo} must be substituted into equation (18a) also. Then, equation (18a) becomes

$$\frac{3\pi^4 D_s Lb}{64(b/n)^4}(3\beta^4+1)\left(\frac{\bar{C}}{h}\right)^2\bar{C} + \frac{3\pi^2 D_s Lb}{4h^2(b/n)^2}\beta^2\left\{\bar{u} + \frac{\pi^2 h^2}{3(b/n)^2}\cdot\frac{(\beta^2+1)^2}{\beta^2[1+n^2\gamma(\beta^2+1)]}\right\}\cdot$$

$$(\bar{C}) = 0 \tag{27}$$

This leads to the critical value of $\bar{u}$,

$$\bar{u}_{cr} = -\frac{\pi^2 h^2}{3(b/n)^2}\cdot\frac{4}{(1+\gamma)^2} \tag{28}$$

when $\bar{C}$ is set to zero, $n = 1$, and $\beta = \sqrt{(1+\gamma)/(1-\gamma)}$. It can be shown here that this is in agreement with $\bar{u}_{cr} = \sigma_{cr}/E$ where $\sigma_{cr} = (N_{xo})_{cr}/2t_f$.

Now, $\bar{C}$, in terms of $\bar{u}$ and $\bar{u}_{cr}$, is

$$\bar{C}^2 = \frac{4(b/n)^2}{\pi^2}\frac{(1-\gamma^2)}{(\gamma^2+\gamma+1)}\cdot\bar{u}_{cr}\left(1 - \frac{\bar{u}}{\bar{u}_{cr}}\right) \tag{29}$$

On the other hand, equation (18i) may be rewritten as

$$N_{xo} = \frac{3D_s}{h^2}\bar{u} + \frac{3\pi^2 D_s}{8(b/n)^2}\beta^2\left(\frac{\bar{C}}{h}\right)^2 \tag{30}$$

Then, with $\bar{C} = 0$ and $\bar{u} = \bar{u}_{cr}$,

$$(N_{xo})_{cr} = \frac{3D_s}{n^2}\bar{u}_{cr} \tag{31}$$

Next, N_x can be expressed in terms of $\bar{u}$ and $\bar{u}_{cr}$ as

$$N_x = \bar{F}\cos\left(\frac{2n\pi y}{b}\right) + N_{xo}$$

or

$$N_x = \frac{3D_s}{2h^2}\frac{(1+\gamma)^2}{(\gamma^2+\gamma+1)}\bar{u}_{cr}\left(\frac{\bar{u}}{\bar{u}_{cr}} - 1\right)\cos\left(\frac{2n\pi y}{b}\right) + N_{xo} \tag{32}$$

Nondimensionalization of N_x with respect to $(N_{xo})_{cr}$ gives

$$\frac{N_x}{(N_{xo})_{cr}} = \frac{(1+\gamma)^2}{2(\gamma^2+\gamma+1)}\left(\frac{\bar{u}}{\bar{u}_{cr}} - 1\right)\cos\left(\frac{2n\pi y}{b}\right) + \frac{N_{xo}}{(N_{xo})_{cr}} \tag{33}$$

But, in view of equations (30) and (31),

$$\frac{N_{xo}}{(N_{xo})_{cr}} = \frac{\bar{u}}{\bar{u}_{cr}} + \frac{(1+\gamma)^2}{2(\gamma^2+\gamma+1)}\left(1 - \frac{\bar{u}}{\bar{u}_{cr}}\right) \tag{34}$$

Finally,

$$\frac{N_x}{(N_{xo})_{cr}} = \frac{(1+\gamma^2)}{2(\gamma^2+\gamma+1)}\left[\left(1 - \frac{\bar{u}}{\bar{u}_{cr}}\right)+\left(\frac{\bar{u}}{\bar{u}_{cr}}\right)\cos\left(\frac{2n\pi y}{b}\right)\right]+ \frac{\bar{u}}{\bar{u}_{cr}} \tag{35}$$

For different values of $\gamma(0, 0.25, 0.5, 1.0)$ and $\bar{u}/\bar{u}_{cr}$ $(1, 2, 10)$, the variation of $N_x/(N_{xo})_{cr}$ across y is shown by the curves in Figure 3. The average value of N_x along the y axis is

$$\frac{(N_x)_{av}}{(N_{xo})_{cr}} = \frac{1}{b}\int_0^b \left\{\frac{(1+\gamma)^2}{2(\gamma^2+\gamma+1)}\left[\left(1 - \frac{\bar{u}}{\bar{u}_{cr}}\right)+\left(\frac{\bar{u}}{\bar{u}_{cr}} - 1\right)\cos\left(\frac{2\pi\gamma y}{b}\right)\right] + \frac{\bar{u}}{\bar{u}_{cr}}\right\} dy$$

$$= \frac{(1+\gamma^2)}{2(\gamma^2+\gamma+1)}\left(1 - \frac{\bar{u}}{\bar{u}_{cr}}\right) + \frac{\bar{u}}{\bar{u}_{cr}}$$

or

$$\frac{(N_x)_{av}}{(N_{xo})_{cr}} = \frac{\gamma^2+1}{2(\gamma^2+\gamma+1)} \cdot \frac{\bar{u}}{\bar{u}_{cr}} + \frac{(1+\gamma)^2}{2(\gamma^2+\gamma+1)} \tag{36}$$

For $\gamma = 0, 0.25, 0.5, 1.0$, the relation between $(N_x)_{av}/(N_{xo})_{cr}$ and $\bar{u}/\bar{u}_{cr}$ is shown graphically in Figure 4.

4. MAXIMUM DEFLECTION

From equation (5), the lateral deflection is

$$w = \bar{C} \sin \frac{m\pi x}{L} \sin \frac{n\pi y}{b}$$

The maximum value occurs at $x = L/2m$ and $y = b/2$. Thus,

$$w_{max} = \bar{C} = \left[\frac{32(1-\gamma)}{3(1+\gamma^2)(1+\gamma)} \left(\frac{N_{xo}}{(N_{xo})_{cr}} - 1\right)\right]^{1/2} h$$

or

$$\frac{w_{max}}{h} = \left[\frac{32(1-\gamma)}{3(1+\gamma^2)(1+\gamma)} \left(\frac{N_{xo}}{(N_{xo})_{cr}} - 1\right)\right]^{1/2} \tag{37}$$

From equation (34), w_{max}/h can be expressed in terms of $\bar{u}/\bar{u}_{cr}$, that is,

$$\frac{w_{max}}{h} = \left[\frac{16(1-\gamma)}{3(1+\gamma)(\gamma^2+\gamma+1)} \cdot \left(\frac{\bar{u}}{\bar{u}_{cr}} - 1\right)\right]^{1/2} \tag{38}$$

Equation (38) agrees with equation (25) when $\bar{C}/h$ is expressed in terms of $\bar{u}/\bar{u}_{cr}$.

For different values of $\gamma(0, 0.25, 0.5, 1.0)$, the variation of w_{max}/h with $\bar{u}/\bar{u}_{cr}$ is shown in Figure 5.

APPENDIX III

PLASTIC ANALYSIS AND NEWTON-RAPHSON ITERATIVE TECHNIQUE

In the plastic case, K is not zero. Therefore, analytic expressions for the assumed displacement and stress coefficients are not obtainable. The Newton-Raphson iterative technique is utilized to obtain the numerical solutions corresponding to vanishing of the first variation of the functional given by equation (3).

In the computer program, it is more convenient to write the functional corresponding to equation (6) for the elastic case in the following form:

$$\frac{U''}{EV} = \int_0^1\int_0^1 \Bigg\{ \frac{\sigma'_x}{E}\epsilon'_x + \frac{\sigma'_y}{E}\epsilon'_y + \frac{\tau'_{xy}}{E}\gamma'_{xy} + \frac{\sigma''_x}{E}\epsilon''_x + \frac{\sigma''_y}{E}\epsilon''_y + \frac{\tau''_{xy}}{E}\gamma''_{xy}$$

$$+ \frac{1}{4}\frac{G_c t_c}{E t_f}(\gamma_{xz}^2 + \gamma_{yz}^2) - \frac{1}{4}\left[\left(\frac{\sigma_{eff}}{E}\right)_t^2 + \left(\frac{\sigma_{eff}}{E}\right)_b^2\right]$$

$$- \frac{K}{2(n+1)}\left[\left(\frac{\sigma_{eff}}{E}\right)_t^{n+1} + \left(\frac{\sigma_{eff}}{E}\right)_b^{n+1}\right]\Bigg\} d\xi\, dn \qquad (39)$$

Programming of this equation constitutes the main subroutine. Also, the following expressions are used in the program. New coefficients, designated by a tilde "~", are introduced. For the elastic portion,

$$\tilde{C} = \frac{\bar{C}}{b/n} = \frac{2}{\pi}\sqrt{\frac{(1-\nu^2)}{(\gamma^2+\gamma+1)}\,\bar{u}_{cr}\left(1 - \frac{\bar{u}}{\bar{u}_{cr}}\right)}$$

$$\tilde{D} = \bar{D} = \frac{\pi n^2\gamma\beta(\beta^2+1)}{[1+n^2\gamma(\beta^2+1)]}\,\tilde{C}$$

$$\tilde{E} = \bar{E} = \frac{\pi n^2\gamma(\beta^2+1)}{[1+n^2\gamma(\beta^2+1)]} \cdot \tilde{C}$$

$$\tilde{F} = \frac{\bar{F}}{Et_f} = -\frac{\pi^2\beta^2}{4} \cdot \tilde{C}^2$$

$$\tilde{G} = \frac{\bar{G}}{Et_f} = -\frac{\pi^2}{4} \cdot \tilde{C}^2$$

$$\tilde{I} = \frac{\bar{I}}{Et_f h} = \frac{\pi^2(2\beta^2+1)}{3[1+n^2\gamma(\beta^2+1)]} \cdot \frac{h}{b/n} \cdot \tilde{C}$$

$$\tilde{J} = \frac{\bar{J}}{Et_f h} = \frac{\pi^2(\beta^2+2)}{3[1+n^2\gamma(\beta^2+1)]} \cdot \frac{h}{b/n} \cdot \tilde{C}$$

$$\tilde{K} = \frac{\bar{K}}{Et_f h} = \frac{\pi^2\beta}{3[1+n^2\gamma(\beta^2+1)]} \cdot \frac{h}{b/n} \cdot \tilde{C}$$

$$\tilde{N}_{xo} = \frac{N_{xo}}{2Et_f} = \bar{u} + \frac{\pi^2\beta^2}{8} \cdot \tilde{C} \qquad (40)$$

It should be noticed that β's here must take the value of $\sqrt{(1+\gamma)/(1-\gamma)}$, so that the coefficients will agree with those taken earlier in the expressions (25) and (29). This is also true for the following expressions. Then, the stresses and strains in equation (39) are

$$\frac{\sigma'_x}{E} = \frac{1}{2}\tilde{F}\cos(\pi\eta) + \tilde{N}_{xo}$$

$$\epsilon'_x = \bar{u} + \frac{1}{2}\beta^2\pi^2\tilde{C}^2\cos^2(\tfrac{\pi}{2}\xi)\cos^2(\tfrac{\pi}{2}\eta)$$

$$\frac{\sigma'_y}{E} = \frac{1}{2}\tilde{G}\cos(\pi\xi)$$

$$\epsilon'_y = \frac{1}{2}\pi^2\tilde{C}^2\sin^2(\tfrac{\pi}{2}\xi)\cos^2(\tfrac{\pi}{2}\eta)$$

$$\frac{\tau'_{xy}}{E}\gamma'_{xy} = 0$$

$$\frac{\sigma''_x}{E} = -\tilde{I}\sin(\tfrac{\pi}{2}\xi)\sin(\tfrac{\pi}{2}\eta)$$

$$\epsilon''_x = \frac{\pi}{2}(\frac{h}{b/n})[-\pi\beta^2\tilde{C} + \beta\tilde{D}]\sin(\tfrac{\pi}{2}\xi)\sin(\tfrac{\pi}{2}\eta)$$

$$\frac{\sigma''_y}{E} = -\tilde{J}\sin(\tfrac{\pi}{2}\xi)\sin(\tfrac{\pi}{2}\eta)$$

$$\epsilon''_y = \frac{\pi}{2}(\frac{h}{b/n})[-\pi\tilde{C} + \tilde{E}]\sin(\tfrac{\pi}{2}\xi)\sin(\tfrac{\pi}{2}\eta)$$

$$\frac{\tau''_{xy}}{E} = \tilde{K}\cos(\tfrac{\pi}{2}\xi)\cos(\tfrac{\pi}{2}\eta)$$

$$\gamma_{xy} = \frac{\pi h}{b/n}[\pi\beta\tilde{C} - \tfrac{1}{2}(\tilde{D} + \beta\tilde{E})]\cos(\tfrac{\pi}{2}\xi)\cos(\tfrac{\pi}{2}\eta)$$

$$\frac{1}{4}\cdot\frac{G_c t_c}{E t_f}(\gamma_{xz}^2 + \gamma_{yz}^2) = \frac{\pi^2}{3}\left(\frac{h}{b/n}\right)^2[\tilde{D}^2\cos^2(\tfrac{\pi}{2}\xi)\sin^2(\tfrac{\pi}{2}\eta) + \tilde{E}^2\sin^2(\tfrac{\pi}{2}\xi)\cos^2(\tfrac{\pi}{2}\eta)]$$

$$\left(\frac{\sigma_{eff}}{E}\right)^2_{t,b} = \left(\frac{\sigma'_x}{E} \pm \frac{\sigma''_x}{E}\right)^2 + \left(\frac{\sigma'_y}{E} + \frac{\sigma''_y}{E}\right)^2 - \left(\frac{\sigma'_x}{E} \pm \frac{\sigma''_x}{E}\right)\left(\frac{\sigma'_y}{E} \pm \frac{\sigma''_y}{E}\right) + 3\left(\frac{\tau'_{xy}}{E} \pm \frac{\tau''_{xy}}{E}\right) \qquad (41)$$

Because of symmetry, the functional integration is performed for a quarter of the plate. For a specified material, for example, one of 2024-T3 aluminum alloy (Figure 5),

$K = 3.14 \times 10^{17}$

$n = 8.6$

$E = 10.7 \times 10^6$ psi

$\sigma_{cy} = 43.6$ ksi

For plate No. 1,

$\sigma_{cr}/\sigma_{cy} = 0.6$

whereas for plate No. 4,

$\sigma_{cr}/\sigma_{cy} = 0.3$

From these given values, $\bar{u}_{cr}$ and h/b are

$$\bar{u}_{cr} = -\frac{\sigma_{cr}}{E}$$

$$\frac{h}{b} = \sqrt{\frac{3\sigma_{cr}}{\pi^2 E(k_x)_{cr}}} = \frac{1+\gamma}{2\pi}\sqrt{\frac{3\sigma_{cr}}{E}}$$

Hence, with assigned values of γ and $\bar{u}/\bar{u}_{cr}$ (elastic case), the stresses and strains at each point can be determined, and the integration of equation (39) can be made numerically by applying Simpson's rule in two dimensions. The corresponding coefficients of the plastic solution can be found numerically by using the elastic-solution coefficients (or known plastic coefficients of a previously calculated neighboring point) as initial values and by applying the Newton-Raphson iterative technique to obtain a stationary value of the functional. This involves the solution of 9 simultaneous nonhomogeneous linear equations.

The functional U''/EV after integration is designed by $\bar{U}''$, and the 9 coefficients of the plastic solution ($\tilde{C}$, $\tilde{D}$, $\tilde{E}$, $\tilde{F}$, $\tilde{G}$, $\tilde{I}$, $\tilde{J}$, $\tilde{K}$, and $\tilde{N}_{xo}$) are designated by x_i. The quantities $\partial\bar{U}''/\partial x_i$ and $\partial^2\bar{U}''/\partial x_i \partial x_j$ are designated by $\bar{U}''_{,i}$ and $\bar{U}''_{,ij}$. Then, the set of equations is

$$\bar{U}''_{,11}\Delta x_1 + \bar{U}''_{,12}\Delta x_2 + \cdots\cdots + \bar{U}''_{,19}\Delta x_9 = -\bar{U}''_{,1}$$

$$\bar{U}''_{,21}\Delta x_2 + \bar{U}''_{,22}\Delta x_2 + \cdots\cdots + \bar{U}''_{,29}\Delta x_9 = -\bar{U}''_{,2}$$

$$- -$$

$$U''_{,9i}\Delta x_1 + U''_{,92}\Delta x_2 + \cdots\cdots + U''_{,99}\Delta x_9 = -U''_{,9}$$

where Δx_i are the unknown increments in the iterative process, and all of the $\bar{U}''_{,i}$, $\bar{U}''_{,ij}$ can be found by the numerical expressions

$$\bar{U}''_{,i} = \frac{\bar{U}''(x_i + \delta x_i) - \bar{U}''(x_i - \delta x_i)}{2\delta x_i}$$

$$\bar{U}''_{,ii} = \frac{\bar{U}''(x_i + \delta x_i) - 2\bar{U}'' + \bar{U}''(x_i - \delta x_i)}{(\delta x_i)^2}$$

$$\bar{U}''_{,ij} = \frac{\bar{U}''(x_i + \delta x_i,\ x_i + \delta x_j) - \bar{U}''(x_i + \delta x_i) - \bar{U}''(x_j + \delta x_j) + \bar{U}''}{\delta x_i \delta x_j}$$

The increments δx_i are taken as $x_i \cdot 10^{-3}$. All of the $\bar{U}''$, $\bar{U}''_i$, $\bar{U}''_{ij}$ are evaluated with the assigned initial coefficients. This involves significant computational effort since different values of γ for the desired range of $\bar{u}/\bar{u}_{cr}$ have to be assigned.

After sufficient iterations, the approximate numerical value of each coefficient can be found to a desired degree of convergence. Then, the stresses and strains at each point of the plate can be calculated. Thus, the average value of σ_x can be determined by numerical integration of the stress distribution across y. The variation of $(\sigma_x)_{av}/(\sigma_x)_{cr}$ (which in this problem is the same as $(N_x)_{av}/(N_{xo})_{cr}$) with respect to the assigned value of $\bar{u}/u_{cr}$ can be plotted in graphical form. This curve determines the load-carrying capability of the sandwich plate in the postbuckling range. Load-shortening curves for plates 1 and 4, with plasticity effects included, are given in Figures 6 and 7, respectively.

With reference to the actual computer programming, it was found that the more digits employed (in Algol W, long real numbers must be used), the better the convergence. The Newton-Raphson iteration technique is basically a very effective method of numerical minimization. However, initially, seven-digit calculations led to a very poor convergence. A simple test program based on a quadratic form in three variables showed that the convergence became remarkably rapid when 15 digits were employed. Of course, since the actual problem reflects 9 arbitrary coefficients and a high degree of nonlinearity in the functional that was varied, convergence was slower but, nevertheless, quite satisfactory.

APPENDIX IV

EFFECTIVE STRESS AND STRAIN

The complementary energy density for linear elastic behavior of plates is (see, for example, Reference 3)

$$F' = \frac{1}{2E}\{\sigma_x^2 + \sigma_y^2 - 2\mu\sigma_x\sigma_y + 2(1+\mu)\gamma_{xy}^2\}$$

This can be easily verified by enforcing the generalized stress-strain relations

$$\left.\begin{aligned} \frac{\partial F'}{\partial \sigma_x} &= \frac{1}{2E}\{2\sigma_x - 2\mu\sigma_y\} = \frac{1}{E}\{\sigma_x - \mu\sigma_y\} = \epsilon_x \\ \frac{\partial F'}{\partial \sigma_y} &= \frac{1}{E}\{\sigma_y - \mu\sigma_x\} = \epsilon_y \\ \frac{\partial F'}{\partial \tau_{xy}} &= \frac{2(1+\mu)}{E}\tau_{xy} = \gamma_{xy} \end{aligned}\right\} \qquad (42)$$

Then, from any one of References 1 through 3,

$$\epsilon_{eff} d\sigma_{eff} = dF' \qquad (43)$$

In linear elasticity, $\sigma_{eff}/\epsilon_{eff} = E$; thus,

$$\int \epsilon_{eff} d\sigma_{eff} = \frac{1}{E}\int \sigma_{eff} d\sigma_{eff} = \int dF' \qquad (44)$$

Integration gives

$$\frac{1}{2E}\sigma_{eff}^2 = F' = \frac{1}{2E}\{\sigma_x^2 + \sigma_y^2 - 2\mu\sigma_x\sigma_y + 2(1+\mu)\gamma_{xy}^2\} \qquad (45)$$

In nonlinear elasticity (References 1 through 3), the same equations hold. For $\mu = 0.5$, the expression for the effective stress is

$$\sigma_{eff} = \sqrt{\sigma_x^2 + \sigma_y^2 - \sigma_x\sigma_y + 3\gamma_{xy}^2} \qquad (46)$$

This expression may be transformed into effective strain simply by using the relations (42), with E replaced by E_s; that is,

$$\sigma_x = \frac{4E_s}{3}(\epsilon_x + \frac{1}{2}\epsilon_y)$$

$$\sigma_y = \frac{4E_s}{3}(\frac{1}{2}\epsilon_x + \epsilon_y) \qquad (47)$$

$$\tau_{xy} = \frac{E_s}{3}\gamma_{xy}$$

and

$$\sigma_{eff} = E_s\epsilon_{eff}$$

Substitution into σ_{eff} gives

$$\epsilon_{eff} = \frac{4}{3}\sqrt{\frac{3}{4}\epsilon_x^2 + \frac{3}{4}\epsilon_y^2 + \frac{3}{4}\epsilon_x\epsilon_y + \frac{3}{16}\gamma_{xy}^2}$$

or

$$\epsilon_{eff} = \frac{2}{\sqrt{3}}\sqrt{\epsilon_x^2 + \epsilon_y^2 + \epsilon_x\epsilon_y + \frac{\gamma_{xy}^2}{4}} \qquad (48)$$

UNCLASSIFIED

Security Classification

DOCUMENT CONTROL DATA - R & D

(Security classification of title, body of abstract and indexing annotation must be entered when the overall report is classified)

1 ORIGINATING ACTIVITY *(Corporate author)*
Stanford University
Department of Aeronautics and Astronautics
Stanford, Calif. 94305

2a. REPORT SECURITY CLASSIFICATION
Unclassified

2b. GROUP
N/A

3. REPORT TITLE

MAXIMUM LOAD PREDICTION FOR SANDWICH PLATES

4. DESCRIPTIVE NOTES *(Type of report and inclusive dates)*

5. AUTHOR(S) *(First name, middle initial, last name)*

J. Mayers and Yuan-shan Chu

6. REPORT DATE	7a. TOTAL NO. OF PAGES	7b. NO. OF REFS
April 1969	49	7

8a. CONTRACT OR GRANT NO	9a. ORIGINATOR'S REPORT NUMBER(S)
DAAJ02-68-C-0035	USAAVLABS Technical Report 69-3
b. PROJECT NO Task 1F162204A17002	
c.	9b. OTHER REPORT NO(S) *(Any other numbers that may be assigned this report)*
d.	SUDAAR No. 366

10. DISTRIBUTION STATEMENT

This document has been approved for public release and sale; its distribution is unlimited.

11. SUPPLEMENTARY NOTES	12. SPONSORING MILITARY ACTIVITY
	U.S. Army Aviation Materiel Laboratories Fort Eusis, Virginia 23604

13. ABSTRACT

An investigation of the postbuckling behavior of sandwich plates compressed beyond the general instability load into the plastic range has been undertaken. The study is a natural extension of previous work which led to the establishment of maximum load-prediction capability relative to conventional plates. The purpose of the present investigation is to assess the effects of transverse shear deformations on the maximum strength of sandwich plates when the primary mode of initial buckling is that of general instability. The analysis utilizes a modified version of Reissner's variational principle and a deformation theory of plasticity in conjunction with computations carried out on high-speed computing equipment. The results indicate that for the particular plate problem investigated (for example, aircraft wing or stabilizer plate element), the postbuckling load-carrying capability is essentially independent of transverse shear effects in the presence of inelastic behavior of the sandwich faces. The implication is that perhaps designers will not have to be as conservative in sizing sandwich plate sections for maximum load-carrying capability as purely elastic theory results would indicate.

DD FORM 1 NOV 68 1473

UNCLASSIFIED

Security Classification

UNCLASSIFIED

Security Classification

14 KEY WORDS	LINK A		LINK B		LINK C	
	ROLE	WT	ROLE	WT	ROLE	WT
Composite Construction						
Sandwich Construction						
Sandwich Plates						
Buckling						
Postbuckling						
Plasticity						
Maximum Strength						
Variational Methods						

UNCLASSIFIED

Security Classification